

Velocity-force characteristics of an interface driven through a periodic potential

A. M. Ettouhami¹ and Leo Radzihovsky^{1,2}

¹*Department of Physics, University of Colorado, Boulder, Colorado 80309*

²*Department of Physics, Harvard University, Cambridge, Massachusetts 02138*

(Received 19 July 2002; published 24 March 2003)

We study creep dynamics of a two-dimensional interface driven through a periodic potential using dynamic renormalization-group methods. We find that the nature of weak-drive transport depends qualitatively on whether the temperature T is above or below the equilibrium roughening transition temperature T_c . Above T_c , the velocity-force characteristics are Ohmic, with linear mobility exhibiting a jump discontinuity across the transition. For $T \leq T_c$, the transport is highly nonlinear, exhibiting an interesting crossover in temperature and weak external force F . For intermediate drive, $F > F_*$, we find near T_c^- a power-law velocity-force characteristics $v(F) \sim F^\sigma$, with $\sigma - 1 \propto \tilde{t}$, and well below T_c , $v(F) \sim e^{-(F_*/F)^{2\tilde{t}}}$, with $\tilde{t} = (1 - T/T_c)$. In the limit of vanishing drive ($F \ll F_*$), the velocity-force characteristics cross over to $v(F) \sim e^{-(F_0/F)}$, and are controlled by soliton nucleation.

DOI: 10.1103/PhysRevB.67.115412

PACS number(s): 05.70.Ln, 64.60.Ht, 64.70.Hz

I. INTRODUCTION

The problem of elastic media pinned by an external potential provides a unifying framework for understanding a large number of condensed-matter phenomena, such as, for example, surface growth,^{1,2} nonlinear transport in anisotropic metals,³ dissipation in superconductors,⁴⁻⁷ Wigner crystals,⁸ earthquakes,⁹ and friction.¹⁰ Randomly pinned elastic systems are also toy models for considerably more complicated problems of glasses.¹¹ Much of the recent interest in such problems has been rekindled by the discovery¹² of high-temperature superconductors (HTSC), and efforts to understand the nature of their B - T phase diagram and dissipation controlled by statics and dynamics of elastic arrays of vortex lines.^{13,4-7} A combination of thermal fluctuations, pinning, and external drive leads to a wide range of different and interesting collective phenomena that are common to many physical realizations of elastic media.⁵⁴

There has been considerable progress in understanding the static properties of pinned elastic media.^{4,14-16} Much of the recent interest has therefore shifted to dynamics, with current focus on nonequilibrium, driven dynamics of these rich systems.⁴⁻⁷ Once the elastic medium is driven, however, many new questions arise, such as the governing nonequilibrium equation of motion, phase classification and stability, nature of the corresponding phase transitions, and the resulting nonequilibrium phase diagram.^{5-7,17,18} Among these many challenging questions, the velocity- (v) force (F) characteristics [the IV curve, in the context of superconductors and charge-density waves (CDW's)] is the observable that is most directly accessible experimentally¹⁹ and is therefore of considerable theoretical interest.

Despite considerable richness of many aspects of the driven state,^{5-7,18-20} at large drives the velocity-force characteristics of a uniformly sliding medium approach Ohmic form with deviations δv that can be computed perturbatively²¹ in the ratio $\delta v/v$. At zero temperature, if elastic,²² the medium is pinned for drives smaller than a critical $T=0$ value F_c , and undergoes a nonequilibrium de-

pinning transition to a sliding state, with $v \sim |F - F_c|^\beta$ playing the role analogous to an order parameter distinguishing pinned and sliding phases.²³ Finite temperature rounds the depinning transition,²⁴ allowing activated creep motion of the elastic solid even for drive far below F_c .

Much of the insight about this highly nontrivial creep regime that is the focus of our work comes from a scaling theory of depinned droplet nucleation.^{13,25-28} This approach generically predicts collectively pinned elastic media to exhibit a highly nonlinear $v(F)$, with a vanishing linear mobility, corresponding to transport activated over barriers that diverge with system size and vanishing drive.²⁹ Recently, in the case of random pinning, these scaling predictions have been put on firmer ground through a detailed dynamic functional renormalization-group (DFRG) calculations of $v(F)$,^{30,31} which indeed predict $v(F) \sim e^{-1/F^\mu}$, with a universal μ exponent. However, in the case of random pinning a number of technical problems with DFRG remain, precluding a fully controlled analysis.^{32,33}

It turns out, however, that many problems of interest, such as surface growth,³⁴ two-dimensional (2D) colloidal crystals in periodic potentials,³⁵⁻³⁸ and vortices pinned by artificial dot arrays³⁹ or by intrinsic pinning in, e.g., HTSC, involve the considerably simpler but still nontrivial problem of *periodic* pinning. In addition to addressing numerous interesting physical problems, study of motion in a periodic potential provides a nice laboratory to explore important calculational methods.

A driven sine-Gordon model is the simplest description of such periodic pinning problem, with an important simplifying feature of absence of topological defects such as dislocations or phase slips that can be important for understanding the dynamics of vortex arrays and CDW's.^{6,40} Directly applicable to crystal-growth phenomena, this model has been extensively studied in the literature.⁴¹⁻⁵⁰ In equilibrium, among many other things, it describes the famous crystal surface roughening transition⁵⁸ from the low-temperature smooth phase with bounded surface roughness to the high-temperature rough phase with logarithmic height correlations.

One of the many interesting questions that naturally arises is: *What are the signatures of the roughening transition in the driven transport?* More specifically, here we are interested in qualitative differences (if any) in $v(F)$ above and below T_c . The equilibrium limit of this question was addressed in the classic analysis of the equilibrium dynamics by Chui and Weeks⁴² and by Nozières and Gallet.⁴⁸ By extending the standard analysis to equilibrium *dynamics*, they found the vanishing of the linear mobility below the roughening transition, consistent with the static picture of the smooth phase where the interface is pinned by the periodic potential.

In the presence of an external drive, the sine-Gordon model was studied sometime ago by Hwa, Kardar, and Paczusi⁵¹ and by Rost and Spohn.⁴⁹ Although these works led to considerable progress, computing the renormalization group (RG) flow equations for model parameters at nonzero F , they concentrated mainly on the influence of Kardar-Parisi-Zhang⁵² (KPZ) nonlinearities (not considered in previous studies⁴⁸) important at strong external drive, but said little about the actual $v(F)$ characteristics of the driven interface in the $F \rightarrow 0$ creep regime. The driven sine-Gordon model has also been considered by Blatter *et al.*⁴ in a complementary approach via a high-velocity perturbative expansion for $v(F)$. Consistent with Refs. 42 and 48, these last authors found that while the correction ($\delta v/v$) remained finite above T_c , it diverged below T_c , thereby suggesting nontrivial transport changes across the roughening transition, but leaving the form of $v(F)$ in the creep regime an open problem. Of course, because at finite temperature the interface can move for any finite drive F , at sufficiently long scales the periodic potential is averaged away at both low and high temperatures, thereby leading to the rounding of the roughening transition itself. Nevertheless, we expect that the velocity-force characteristics in the *creep* regime are controlled by the equilibrium physics and precise qualitative distinction of $v(F)$ in the rough and smooth phases should exist.^{53,55}

In this paper, our goal is to understand in detail the physical consequences of the divergences found in the high-velocity perturbative expansion and in particular to compute the creep velocity-force characteristics in both phases and across the roughening transition, utilizing dynamic RG.^{6,30-33} Consistent with perturbative analysis, we find that the nature of transport depends qualitatively on whether the temperature is above or below the equilibrium roughening transition temperature T_c . Above T_c , the velocity-force characteristics are Ohmic, with the mobility remaining finite for $T \rightarrow T_c^+$. In contrast, for $T < T_c$, we find that the linear mobility vanishes on long-length scales, and therefore exhibits a nonuniversal jump discontinuity across the roughening transition.^{48,49,4} In the smooth phase, the transport is a strongly nonlinear function of applied force, showing a rich universal crossover in temperature and applied force (Fig. 1). At an intermediate drive $F > F_*(\bar{g}, T)$, larger than the pinning- (\bar{g}) and temperature-dependent strong-coupling crossover force

$$F_*(\bar{g}, T) \sim \begin{cases} e^{-b_1/\bar{g}^2}, & T \rightarrow T_c^- \\ \bar{g}^{1/\tilde{t}}, & T \ll T_c \end{cases} \quad (1.1)$$

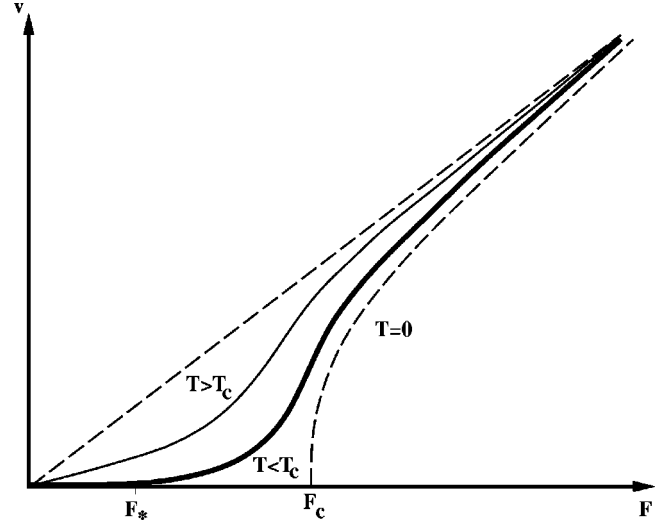


FIG. 1. Typical velocity-force characteristics of a driven interface in a periodic potential. At zero temperature, the interface remains pinned ($v=0$) until F reaches the critical force $F_c=pg$. At finite temperatures, we find that the near-equilibrium response of the interface to a small ($F \ll F_c$) driving force depends on whether T is above or below the roughening temperature T_c . For $T > T_c$, the velocity-force characteristics are Ohmic [$v(F) \sim F$] down to $F=0$, while for $T < T_c$ and forces smaller than a characteristic force F_* , the characteristics are strongly nonlinear, $v \sim \exp(-F_0/F)$, creep motion via activation over barriers that diverge in a vanishing drive limit.

the velocity-force characteristics strongly depend on the level of proximity to T_c , with

$$v(F) \sim \begin{cases} F^{(1+b_2\tilde{t})}, & T \rightarrow T_c^- \\ e^{-(F_*/F)^{2\tilde{t}}}, & T \ll T_c, \end{cases} \quad (1.2)$$

where $\tilde{t} = (1 - T/T_c)$, and b_1 and b_2 are nonuniversal constants of order unity. For sufficiently low drive $F < F_*(\bar{g}, T)$, the motion is instead always via activated soliton creep, with the velocity-force characteristics crossing over to

$$v(F) \sim e^{-F_0/F}, \quad F < F_*, \quad (1.3)$$

with F_0 another characteristic force that will be defined below, Eq. (5.17).

This paper is organized as follows. We introduce the driven sine-Gordon model in Sec. II and analyze it in Sec. III using simple perturbation theory in the pinning potential strength. While for weak pinning this computation is convergent for $T > T_c$, it fails for arbitrarily weak pinning in the smooth phase. In Sec. IV we employ dynamic RG techniques to make sense of these divergences, and in Sec. V, we use these results to compute $v(F)$ through the roughening transition. We conclude in Sec. VI with a summary of the results and a discussion of open problems and future directions.

II. DRIVEN SINE-GORDON MODEL

In equilibrium, a two-dimensional sine-Gordon model of an elastic interface is described by a Hamiltonian

$$H = \int d\mathbf{r} \left[\frac{1}{2} K (\nabla h)^2 - g \cos[ph(\mathbf{r})] \right], \quad (2.1)$$

where \mathbf{r} is a two-dimensional vector in the (xy) plane, $h(\mathbf{r})$ is the height of the interface above the (xy) plane (taken to be along the z direction in the embedding space) at location \mathbf{r} , K is the interfacial surface tension, g is the pinning strength, and $d = 2\pi/p$ is the period of the potential. In the context of a crystalline surface, with H characterizing its equilibrium roughness, the periodic pinning potential softly encodes lattice periodicity of the bulk crystal, corresponding to the $h \rightarrow h + d$ a symmetry of the surface energy, with d being the crystal lattice constant perpendicular to the interface.

In the absence of any additional conservation laws, long-scale equilibrium dynamics can be described by a simple, relaxational (model A) Langevin equation

$$\begin{aligned} \gamma \partial_t h &= - \frac{\delta H}{\delta h(\mathbf{r}, t)} + \zeta(\mathbf{r}, t) \\ &= K \nabla^2 h(\mathbf{r}, t) - pg \sin[ph(\mathbf{r}, t)] + \zeta(\mathbf{r}, t), \end{aligned} \quad (2.2)$$

where γ is the microscopic friction coefficient, and $\zeta(\mathbf{r}, t)$ a zero-mean, Gaussian thermal noise describing the interaction of the system with the surrounding heat bath at temperature T , with

$$\langle \zeta(\mathbf{r}, t) \zeta(\mathbf{r}', t') \rangle = 2\gamma T \delta(\mathbf{r} - \mathbf{r}') \delta(t - t'), \quad (2.3)$$

in equilibrium imposed by the fluctuation-dissipation theorem (FDT), forbidding independent renormalization of T .

The dynamic description of an interface driven by an external force F (in the context of crystal growth proportional to the difference between the chemical potentials of the solid and vapor phases) is substantially modified. In addition to the obvious addition of the driving force F on the right-hand side of Eq. (2.2), nonequilibrium dynamics permits the appearance of nonconservative forces (those not expressible as derivatives of H), the most important of which is the famous KPZ $(\nabla h)^2$ nonlinearity,⁵² allowed by the explicit breaking by the drive of the $z \rightarrow -z$ symmetry. An additional important effect of driving appears as the renormalization of “temperature” T , corresponding to the breakdown of the fluctuation-dissipation theorem, that is, the renormalization of the friction coefficient γ is independent of that of the variance of the noise ξ . Even if these nonequilibrium effects are not recognized *a priori*, they appear upon coarse graining of Eq. (2.2) as soon as the external drive F is included.⁶³ The resulting nonequilibrium equation of motion is given by⁴⁹

$$\gamma \partial_t h = K \nabla^2 h + \frac{\lambda}{2} (\nabla h)^2 - pg \sin[ph(\mathbf{r}, t)] + F + \zeta(\mathbf{r}, t). \quad (2.4)$$

Our goal here is to apply the machinery of the dynamic RG to compute the velocity-force $v(F)$ characteristics for the above model, focusing on the nontrivial creep regime of the smooth phase, where naive perturbative expansion in the pinning potential g fails.

III. DYNAMIC PERTURBATION THEORY

It is instructive to first study the velocity-force characteristics through a simple perturbative expansion in the pinning potential g . Starting from Eq. (2.4), it is convenient to shift $h(\mathbf{r}, t) = v_0 t + u(\mathbf{r}, t)$ with $v_0 = F/\gamma$ the unperturbed ($g = \lambda = 0$) expression of the velocity. Averaging Eq. (2.4) over thermal fluctuations, and ignoring the KPZ term, we find that the velocity v of the moving interface is given by

$$v = \langle \partial_t h \rangle \quad (3.1a)$$

$$= \frac{F}{\gamma} - \frac{pg}{\gamma} \langle \sin[pu(\mathbf{r}, t) + pv_0 t] \rangle, \quad (3.1b)$$

where we used the fact that $\langle \zeta(\mathbf{r}, t) \rangle = 0$. We now let

$$u(\mathbf{r}, t) = u_0(\mathbf{r}, t) + u_g(\mathbf{r}, t), \quad (3.2)$$

where

$$u_0(\mathbf{r}, t) = \int d\mathbf{r}' dt' R_0(\mathbf{r} - \mathbf{r}', t - t') \zeta(\mathbf{r}', t') \quad (3.3)$$

is the thermal (noninteracting) part of the interface displacement,

$$\begin{aligned} u_g(\mathbf{r}, t) &= pg \int d\mathbf{r}' dt' R_0(\mathbf{r} - \mathbf{r}', t - t') \\ &\quad \times \sin\left(\frac{pFt'}{\gamma} + pu_0(\mathbf{r}', t')\right) \end{aligned} \quad (3.4)$$

is the correction to u linear in the pinning potential strength g , and $R_0(\mathbf{r} - \mathbf{r}', t - t') = \delta\langle u_0(\mathbf{r}, t) \rangle / \delta F(\mathbf{r}', t')$ is the response function of the free interface.⁵⁷ Expanding Eq. (3.1b) in u_g , and averaging over the thermal noise ζ , we find (see also Sec. 2 of the Appendix)

$$\begin{aligned} v &= \frac{F}{\gamma} - \frac{p^3 g^2}{2\gamma} \int d\mathbf{r}' dt' e^{-(1/2)p^2 C_0(\mathbf{r} - \mathbf{r}', t - t')} \\ &\quad \times \sin\left[\frac{pF}{\gamma}(t - t')\right] R_0(\mathbf{r} - \mathbf{r}', t - t'), \end{aligned} \quad (3.5)$$

where $C_0(\mathbf{r} - \mathbf{r}', t - t') = \langle [u_0(\mathbf{r}, t) - u_0(\mathbf{r}', t')]^2 \rangle$ is the connected correlation function of a free interface given by

$$C_0(\mathbf{r}, t) \approx \frac{T}{2\pi K} \ln \left[1 + \Lambda^2 \left(r^2 + \frac{Kt}{\gamma} \right) \right]. \quad (3.6)$$

The above velocity-force characteristics, Eq. (3.5), is most easily evaluated at zero temperature where $C_0(\mathbf{r}, t) = 0$. In this limit, using

$$R_0(\mathbf{r}, t) = \frac{\theta(t)}{\gamma} \int_{\mathbf{q}}^{\Lambda} e^{-Kq^2 t / \gamma} e^{i\mathbf{q} \cdot \mathbf{r}}, \quad (3.7)$$

[$\theta(t)$ is Heaviside's unit step function] in Eq. (3.5) and integrating over the time variable t' , we obtain

$$v = \frac{F}{\gamma} - \frac{p^3 g^2}{2\gamma} \int d\mathbf{r} \int_{\mathbf{q}}^{\Lambda} \frac{pF}{K^2 q^4 + p^2 F^2} e^{i\mathbf{q} \cdot \mathbf{r}}. \quad (3.8)$$

In the above equations and throughout the rest of this paper, we use a shorthand notation $\int_{\mathbf{q}}$ for $\int d\mathbf{q}/(2\pi)^2$, and the superscript $\Lambda = 2\pi/a$ is the ultraviolet cutoff set by the in-plane lattice constant a , generically distinct from the period $d = 2\pi/p$ perpendicular to the interface. Performing the integration over the space variable \mathbf{r} in the last equation, and using the resulting Dirac δ function $(2\pi)^2 \delta(\mathbf{q})$ to complete the \mathbf{q} integral, we find a $T=0$, leading order (in pinning g) expression for the $v(F)$ characteristics^{4,59,21}

$$v = \frac{F}{\gamma} \left[1 - \frac{1}{2} \left(\frac{F_c}{F} \right)^2 \right], \quad F \gg F_c, \quad (3.9)$$

where $F_c = pg$ is the zero-temperature critical force, in agreement with the condition $F_c = \max|\partial V(h)/\partial h|$ of disappearance of metastability [$V(h) = -g \cos(ph)$ is the pinning potential]. As is clear from this result for $v(F)$, even at $T=0$, the perturbative corrections are small for sufficiently large applied force F relative to the pinning force F_c (equivalently, for sufficiently weak pinning g at fixed F). In this fast moving regime, the metastability is absent and pinning gives only a small correction to the motion with $v(F)$ deviating only weakly from the pinning-free Ohmic response $v_0(F) = F/\gamma$. It is reassuring to note that, since at $T=0$, only the $\mathbf{q}=0$ mode contributes to the $v(F)$, Eq. (3.9) agrees with the high-drive limit of the *exact* $T=0$ result^{60,61} for a single particle driven through a one-dimensional sinusoidal potential

$$v(F) = \frac{F}{\gamma} \sqrt{1 - \left(\frac{F_c}{F} \right)^2}, \quad F > F_c. \quad (3.10)$$

This suggests that the $v(F)$ characteristics of a driven interface should also exhibit a square-root cusp with an infinite slope at $F = F_c$. At $T=0$, the interface is strictly pinned for $F \leq F_c$.

In contrast, at any finite temperature the interface moves for arbitrarily weak force and hence there is no sharp depinning transition. The perturbative expression for v , Eq. (3.5) can be readily evaluated by using the fluctuation-dissipation relation

$$\theta(t) \partial_t C_0(\mathbf{r}, t) = 2TR_0(\mathbf{r}, t) \quad (3.11)$$

obeyed by the equilibrium response and correlation functions. Using this relation to eliminate $R_0(\mathbf{r}, t)$ from the right-hand side (rhs) of Eq. (3.5) and integrating by parts over t' we find

$$v = \frac{F}{\gamma} \left[1 - \frac{p^2 g^2}{2\gamma T} \int d\mathbf{r} \int_0^\infty dt \cos(pFt/\gamma) e^{-(1/2)p^2 C_0(\mathbf{r}, t)} \right]. \quad (3.12)$$

Inserting into this last equation, the expression of the correlation function $C_0(\mathbf{r}, t)$ of a harmonic interface given in Eq. (3.6) leads to

$$v = \frac{F}{\gamma} \left(1 - \frac{p^2 g^2}{2\gamma T} \int d\mathbf{r} \int_0^\infty dt \frac{\cos(pFt/\gamma)}{[1 + \Lambda^2(r^2 + Kt/\gamma)]^\eta} \right), \quad (3.13)$$

where we defined

$$\eta = \frac{Tp^2}{4\pi K}. \quad (3.14)$$

Taking the limit $F \rightarrow 0$ in the above expression, and performing the time integration, we obtain

$$\lim_{F \rightarrow 0} (v/F) = \frac{1}{\gamma} \left(1 - \frac{\pi p^2 g^2}{KT\Lambda^3} \int_0^\infty \frac{dr}{(1 + \Lambda^2 r^2)^{(2\eta-3)/2}} \right). \quad (3.15)$$

We now observe that the integral on the rhs of Eq. (3.15) behaves very differently depending on whether T is smaller or greater than

$$T_{c0} = \frac{8\pi K}{p^2}. \quad (3.16)$$

For $T > T_{c0}$, i.e., $\eta > 2$, the integral in Eq. (3.15) is convergent, and leads to a finite (and for weak pinning g , to an arbitrarily small) correction to the linear friction coefficient $\gamma(F=0) = 1/\lim_{F \rightarrow 0} (v/F)$. In strong contrast, for $T < T_{c0}$ ($\eta < 2$) above integral diverges signalling the breakdown of the perturbation theory at small values of the external force F .

Having established the breakdown of perturbation theory for $T < T_{c0}$ in the limit of vanishingly small forces, we now turn our attention to the full velocity-force characteristics at finite values of the external drive. Starting from Eq. (3.13), and performing the integration over space variables, we obtain

$$v = \frac{F}{\gamma} \left(1 - \frac{p^4 g^2}{8K^2 \Lambda^4} \frac{\eta}{\eta-1} \int_0^\infty d\tau \frac{\cos(2f\tau)}{(\tau+1)^{\eta-1}} \right), \quad (3.17)$$

where the dimensionless force f is given by (henceforth, we shall use both F and f to designate the driving force on our interface)

$$f = \frac{pF}{2K\Lambda^2}. \quad (3.18)$$

Performing the integral⁶² on the rhs of Eq. (3.17), we finally arrive at the following result for the effective friction coefficient $\gamma(f)$ of the driven interface (here ${}_1F_2$ is a generalized hypergeometric function):

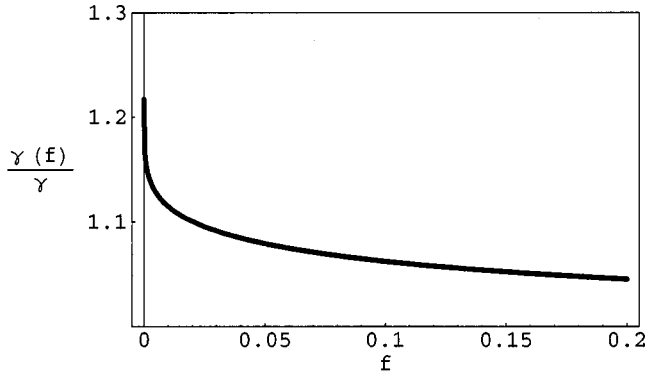


FIG. 2. Effective friction coefficient $\gamma(f)$ of the driven interface for $\eta=2.2$ and $(p^4g^2/8K^2\Lambda^4)=0.02$. As $f \rightarrow 0$, $\gamma(f)$ remains finite, in agreement with Eq. (3.21).

$$\gamma(f) = \gamma \left\{ 1 - \frac{p^4g^2}{8K^2\Lambda^4} \frac{\eta}{\eta-1} \left[(2f)^{\eta-2} \Gamma(2-\eta) \times \sin\left(2f + \frac{\pi}{2}(\eta-1)\right) + \frac{1}{(\eta-2)!} F_2\left(1; \frac{4-\eta}{2}, \frac{3-\eta}{2}; -f^2\right) \right] \right\}^{-1}, \quad (3.19)$$

which has the following limiting behavior as $f \rightarrow 0$,

$$\gamma(f \rightarrow 0) = \gamma \left\{ 1 + \frac{p^4g^2}{8K^2\Lambda^4} \frac{\eta}{(2-\eta)(\eta-1)} \times \left[1 - (2-\eta)\Gamma(2-\eta)(2f)^{\eta-2} \sin\left(\frac{\pi}{2}(\eta-1)\right) \right] \right\}^{-1}. \quad (3.20)$$

As found above, inside the rough phase, $T > T_{c0}$ ($\eta > 2$) and for sufficiently weak pinning, the perturbation theory remains valid at arbitrary f , simply displaying crossover from a freely moving interface with “bare” mobility $\mu_\infty = 1/\gamma$ at high drives to that with *finitely* suppressed low-drive mobility (as illustrated in Fig. 2):

$$\gamma(f \rightarrow 0) \approx \gamma \left(1 + \frac{p^4g^2}{8\eta K^2\Lambda^4} \right) = \gamma \left(1 + \frac{\pi p^2g^2}{2TK\Lambda^4} \right). \quad (3.21)$$

On the other hand, in agreement with Ref. 4, we find that in the “smooth,” low-temperature $T < T_c$ ($\eta < 2$) phase, the behavior is strikingly different with the correction to $v_0(F) = F/\gamma$, Eq. (3.20), diverging and the perturbative approach failing as f is reduced below a characteristic force

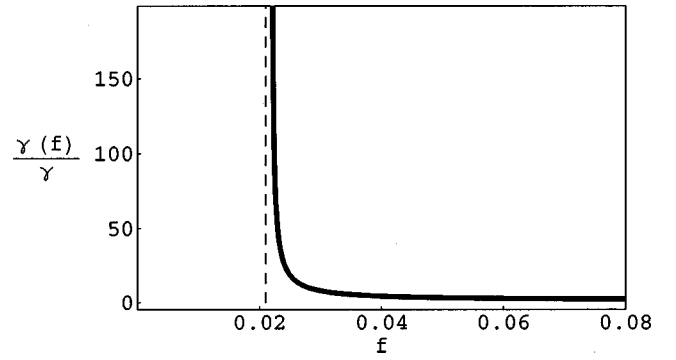


FIG. 3. Effective friction $\gamma(f)$ for $\eta=1.8$ and $(p^4g^2/8K^2\Lambda^4) = 0.1$. $\gamma(f)$ diverges at $f_* \approx 0.022$ (dashed line), indicating the failure of perturbation theory at small drives $0 < f < f_*$.

$$f_*(g, T) \approx \frac{1}{2} \left[\frac{\frac{p^4g^2}{8K^2\Lambda^4} \frac{\eta\Gamma(2-\eta)}{(\eta-1)} \sin\left[\frac{\pi}{2}(\eta-1)\right]}{1 + \frac{p^4g^2}{8K^2\Lambda^4} \frac{\eta}{(2-\eta)(\eta-1)}} \right]^{1/(2-\eta)}. \quad (3.22)$$

As $T \rightarrow T_{c0}^-$ ($\eta \rightarrow 2^-$),

$$f_*(T_{c0}^-) \approx \frac{1}{2} \exp\left(-\frac{4K^2\Lambda^4}{p^4g^2}\right), \quad (3.23)$$

showing that the regime of forces $0 < f < f_*$ where perturbation theory fails becomes exponentially small as T_{c0} is approached from below. The unbounded growth of the perturbative friction coefficient as the external drive f approaches f_* from above (see Fig. 3) suggests that the interface in the low-temperature, smooth phase is characterized by a vanishing linear mobility.^{48,4}

Although we will study this in more detail in following sections, already at this stage we can see a physical interpretation of this divergence. Perturbation theory in the pinning potential fails because even for an arbitrarily weak pinning g , on sufficiently long scales greater than ξ (computed in Sec. IV), the periodic potential (for small h acting like a “mass,” $\frac{1}{2}gp^2h^2$) necessarily dominates over the elastic energy density $(K/2)(\nabla h)^2$. Since [as is quite clear from the equation of motion, Eq. (2.4)] the applied force F dominates the elastic force on scales longer than

$$\xi_F = \left(\frac{2\pi K}{pF} \right)^{1/2}, \quad (3.24)$$

a sufficiently weak force, $F < F_*$, probes the interface on length scales longer than ξ and thereby leads to the breakdown of perturbation theory about the harmonic interface. Hence, although quite instructive, the perturbation theory fails to make predictions for $v(F)$ or any other dynamic quantity in the smooth phase at sufficiently low drive $F < F_*$ and a nonperturbative approach is necessary.

IV. DYNAMIC RENORMALIZATION GROUP

Armed with the above discussion, we are now well equipped to use dynamic RG analysis to make physical sense of these perturbative divergences, with the main goal being the calculation of $v(F)$ in the smooth $T < T_c$ phase for weak drive $F < F_*$. It is convenient to perform this analysis in the frame comoving with the bare velocity $v_0 = F/\gamma$ corresponding to the change of the dynamic fields to $u(\mathbf{r}, t) \equiv h(\mathbf{r}, t) - Ft/\gamma$, which obeys

$$\gamma \partial_t u = K \nabla^2 u + \frac{\lambda}{2} (\nabla u)^2 + pg \sin\left(pu + \frac{pF}{\gamma} t\right) + \zeta(\mathbf{r}, t). \quad (4.1)$$

Taking the nonlinear terms in the above equation as a small perturbation, the equation of motion can be directly expanded in these nonlinearities^{64–66} leading to renormalization-group recursion relations for model parameters. An equivalent but more convenient formulation is the field-theoretic approach of Martin, Siggia, and Rose⁶⁷ (MSR). In this approach, the dynamic correlation and response functions,

$$C(\mathbf{r}, t) = \langle u(\mathbf{r}, t) u(\mathbf{0}, 0) \rangle = \int [du][d\bar{u}] u(\mathbf{r}, t) u(\mathbf{0}, 0) e^{-S[u, \bar{u}]}, \quad (4.2a)$$

$$R(\mathbf{r}, t) = \langle \bar{u}(\mathbf{r}, t) u(\mathbf{0}, 0) \rangle = \int [du][d\bar{u}] \bar{u}(\mathbf{r}, t) u(\mathbf{0}, 0) e^{-S[u, \bar{u}]}, \quad (4.2b)$$

are computed directly by integrating over the phonon and response fields u and \bar{u} , treated as independent stochastic fields with a statistical weight $e^{-S[u, \bar{u}]}$ imposed by the equation of motion, after integrating over the thermal noise $\zeta(\mathbf{r}, t)$. The resulting effective “action” S is given by $S = S_0 + S_1$, where

$$S_0[u, \bar{u}] = \int d\mathbf{r} dt \left\{ \frac{1}{2} (2\gamma T) \bar{u}^2(\mathbf{r}, t) + i\bar{u}(\mathbf{r}, t) [\gamma \partial_t u - K \nabla^2 u] \right\} \quad (4.3)$$

is the action of a pinning-free (harmonic) interface, and where $S_1 = S_g + S_\lambda$, with

$$S_g[u, \bar{u}] = pg \int d\mathbf{r} dt i\bar{u}(\mathbf{r}, t) \sin\left(pu(\mathbf{r}, t) + \frac{pFt}{\gamma}\right) \quad (4.4)$$

the contribution of the pinning potential and

$$S_\lambda[u, \bar{u}] = -\frac{\lambda}{2} \int d\mathbf{r} dt i\bar{u}(\mathbf{r}, t) (\nabla u)^2 \quad (4.5)$$

the contribution of the KPZ term to the nonlinearities in S . To study the renormalization of $S[u, \bar{u}]$, it is sufficient to work with the dynamic “partition function”

$$\mathcal{Z} = \int [du][d\bar{u}] e^{-S[u, \bar{u}]}, \quad (4.6)$$

required to remain fixed at unity under an RG coarse-graining procedure. The advantage of the MSR formalism is its close resemblance to the equilibrium statistical mechanics, which makes it a rather straightforward task to apply RG transformations and to derive recursion relations for the various parameters entering the equation of motion (4.1). Like the static momentum-shell RG, the dynamic RG procedure consists of three main steps,

(i) Thinning of the degrees of freedom, whereby modes $u(\mathbf{q})$, with \mathbf{q} in an infinitesimal shell $\Lambda/b < q < \Lambda$ ($b = e^{d\ell}$) are perturbatively (in S_1) integrated out.

(ii) Rescaling of space variables according to $\mathbf{r} = b\mathbf{r}'$, so as to restore (for convenience) the ultraviolet cutoff to its original value Λ , and rescaling time variable according to $t = t' b^z$.

(iii) Rescaling of fields, in order (for convenience) to keep the harmonic part of the action invariant under rescaling in (ii).

We define “slow” $\{u^<, \bar{u}^<\}$ and “fast” fields $\{u^>, \bar{u}^>\}$

$$u(\mathbf{q}, t) = u^<(\mathbf{q}, t) + u^>(\mathbf{q}, t), \quad (4.7)$$

$$\bar{u}(\mathbf{q}, t) = \bar{u}^<(\mathbf{q}, t) + \bar{u}^>(\mathbf{q}, t), \quad (4.8)$$

with momentum support in Fourier space in the intervals $0 < q < \Lambda/b$ and $\Lambda/b < q < \Lambda$, respectively, and perform a cumulant expansion of \mathcal{Z} in terms of $S_1[u, \bar{u}]$, considered as a perturbation,

$$\begin{aligned} \mathcal{Z} &= \int [du][d\bar{u}] e^{-S_0[u^<, \bar{u}^<]} \langle e^{-S_1[u, \bar{u}]} \rangle_{0>} \\ &\simeq \int [du][d\bar{u}] e^{-S_0[u^<, \bar{u}^<] - \langle S_1 \rangle_{0>} + (1/2) \langle S_1^2 \rangle_{0>}^c}, \end{aligned} \quad (4.9)$$

where $\langle \dots \rangle_{0>}$ denotes an average taken with the statistical weight $S_0[u^<, \bar{u}^<]$, and where the superscript c in $\langle S_1^2 \rangle_{0>}^c$ denotes a connected average. To first order in the pinning strength g , there is only one term in $\langle S_g \rangle_{0>}^c$, which renormalizes the dynamic action S , namely,

$$\langle S_g \rangle_{0>}^c \simeq pg b^{-Tp^2/4\pi K} \int d\mathbf{r} dt i\bar{u}^<(\mathbf{r}, t) \sin\left(pu^<(\mathbf{r}, t) + \frac{pFt}{\gamma}\right), \quad (4.10)$$

which physically arises from the suppression (from g to $g b^{-Tp^2/4\pi K}$) of the effective pinning strength due to short-scale thermal fluctuations averaging away the periodic potential. In the above and throughout, we will use \equiv to indicate that only the leading term has been kept. Similarly, to first order in the KPZ coupling λ , we have the following perturbative correction to the dynamic action S :

$$\langle S_\lambda \rangle_{0>}^c \simeq - \int d\mathbf{r} dt i\bar{u}^<(\mathbf{r}, t) \left[\frac{\lambda T \Lambda^2}{4\pi K} d\ell \right], \quad (4.11)$$

which quite clearly renormalizes the effective external force.

Rescaling the space and time variables

$$\mathbf{r} = b \mathbf{r}', \quad (4.12a)$$

$$t = b^z t', \quad (4.12b)$$

as well as the conjugate field $\tilde{u}(\mathbf{r}, t)$,

$$\tilde{u}^<(\mathbf{r}, t) = b^{\hat{\chi}} \tilde{u}(\mathbf{r}', t'), \quad (4.13)$$

while for convenience leaving $u(\mathbf{r}, t)$ unchanged in order to preserve the periodicity ($2\pi/p$) of the original problem,⁶⁸ we obtain the following lowest-order recursion relations:

$$(\gamma T)(b) = b^{2+z+2\hat{\chi}} (\gamma T), \quad (4.14a)$$

$$\gamma(b) = b^{2+\hat{\chi}} \gamma, \quad (4.14b)$$

$$K(b) = b^{z+\hat{\chi}} K, \quad (4.14c)$$

$$g(b) = b^{2+z+\hat{\chi}-Tp^2/4\pi K} g, \quad (4.14d)$$

$$\lambda(b) = b^{z+\hat{\chi}} \lambda, \quad (4.14e)$$

$$(F/\gamma)(b) = b^z (F/\gamma). \quad (4.14f)$$

The dynamic exponents z and $\hat{\chi}$ can be fixed by requiring that K and γ be unchanged, to linear order in g , under the RG transformation. This leads to the following values:

$$z = 2, \quad \hat{\chi} = -2$$

and to the following recursion relations for g and F ,

$$\frac{dg}{d\ell} = \left(2 - \frac{Tp^2}{4\pi K} \right) g, \quad (4.15a)$$

$$\frac{dF}{d\ell} = 2F + \frac{\lambda T \Lambda^2}{4\pi K}, \quad (4.15b)$$

while the remaining quantities, K , γ , λ , and temperature T , remain unchanged and suffer no renormalization to first order in g and λ . Similar considerations, with details given in Sec. 2 of the Appendix, lead to the following recursion relations to second order in g and λ :

$$\frac{d}{d\ell} (\gamma T) = \left[\frac{T\lambda^2}{8\pi K^3} + \frac{Tp^6 g^2}{16\pi K^3 \Lambda^4} \frac{1}{1+f^2} \right] (\gamma T), \quad (4.16a)$$

$$\frac{d\gamma}{d\ell} = \frac{Tp^6 g^2}{16\pi K^3 \Lambda^4} \frac{1-f^2}{(1+f^2)^2} \gamma, \quad (4.16b)$$

$$\frac{dg}{d\ell} = \left(2 - \frac{Tp^2}{4\pi K} \right) g, \quad (4.16c)$$

$$\frac{dK}{d\ell} = \frac{Tp^6 g^2}{16\pi K^2 \Lambda^4} \frac{2-3f^2-f^4}{(1+f^2)^3}, \quad (4.16d)$$

$$\frac{d\lambda}{d\ell} = \frac{Tp^7 g^2}{16\pi K^2 \Lambda^4} \frac{f(f^2+5)}{(1+f^2)^3}, \quad (4.16e)$$

$$\frac{dF}{d\ell} = 2F + \frac{\lambda T \Lambda^2}{4\pi K} - \frac{Tp^5 g^2}{8\pi K^2 \Lambda^2} \frac{f}{1+f^2}, \quad (4.16f)$$

where $f = (pF/2K\Lambda^2)$ is the dimensionless force of Eq. (3.18). Note that, because of the lack of a FDT for the driven system, in strong contrast to the equilibrium case ($\lambda = F = 0$), Eqs. (4.16a) and (4.16b) imply that $T(\ell)$ flows non-trivially according to

$$\frac{dT}{d\ell} = \left[\frac{T\lambda^2}{8\pi K^3} + \frac{Tp^6 g^2}{8\pi K^3 \Lambda^4} \frac{f^2}{(1+f^2)^2} \right] T. \quad (4.17)$$

Hence, $T(\ell)$ is simply a measure of the strength of the white-noise component of the random force on the driven interface and is not associated with any equilibrium bath at a well-defined thermodynamic temperature.

The recursion relations (4.16a)–(4.16f) contain most (but not all, as discussed in Sec. V) of the information we need to investigate the properties of the system beyond the failing perturbative expansion of Sec. III. Before turning to their full analysis and to the study of the velocity-force characteristics, it is useful to see how the previously derived static and equilibrium dynamic results^{48,56,69} are recovered. We do this in the following sections.

A. Analysis of the static limit

The static model, Eq. (2.1), is characterized by two parameters K and g with the RG recursion relations reducing to the familiar Kosterlitz-Thouless form (derived by these last authors in a dual, Coulomb gas form⁷⁰)

$$\frac{dg}{d\ell} = \left(2 - \frac{Tp^2}{4\pi K} \right) g, \quad (4.18a)$$

$$\frac{dK}{d\ell} = \frac{Tp^6 g^2}{8\pi K^2 \Lambda^4}. \quad (4.18b)$$

At small g , $K(\ell)$ flows slowly, and the recursion relation for g implies the existence of a phase transition (called “roughening” in the context of crystal surface⁴²) at $T_{c0} = 8\pi K/p^2$ (in the limit $g \rightarrow 0$) between two phases distinguished by the long-scale ($\ell \rightarrow \infty$) behavior of $g(\ell)$. For $T > T_{c0}$, thermal fluctuations are strong enough to effectively average away the long-length scale effects of the periodic pinning potential, which is therefore qualitatively unimportant for most (but not all) physical properties of this so-called “rough” phase. At these high temperatures, the surface is logarithmically rough and the effects of a weak periodic potential can be taken into account in a controlled perturbative expansion. In strong contrast, for $T < T_{c0}$, the effective strength of the periodic potential relative to that of the harmonic elastic energy grows on long-length scales, leading to a breakdown of perturbation theory in g , no matter how weak its bare value might be. As a result, at long scales, the interface is pinned in this “smooth” phase, with bounded rms height fluctuations.

It is instructive to recall some of the physics which follows from the above recursion relations. It is convenient to first rewrite the flow equations for dimensionless couplings \tilde{g} and η ,

$$\tilde{g} = \frac{\sqrt{2}p^2g}{K\Lambda^2}, \quad (4.19a)$$

$$\eta = \frac{Tp^2}{4\pi K}, \quad (4.19b)$$

which satisfy

$$\frac{d\tilde{g}}{d\ell} = (2 - \eta)\tilde{g}, \quad (4.20)$$

$$\frac{d\eta}{d\ell} = -\frac{1}{4}\eta^2\tilde{g}^2. \quad (4.21)$$

These show that in equilibrium, the quantity η which is the measure of the ratio of thermal (T) to elastic (K) energy, always flows to zero at long scales, indicating that the low-temperature smooth phase is controlled by a strong coupling zero-temperature fixed point. Near T_c , it is convenient to use a reduced temperature measured relative to the (noninteracting) $T_{c0} = 8\pi K/p^2$,

$$\tilde{\tau} \equiv \eta - 2 \quad (4.22a)$$

$$= 2(T/T_{c0} - 1), \quad (4.22b)$$

with the flow equations simplifying to

$$\frac{d\tilde{g}}{d\ell} = -\tilde{\tau}\tilde{g}, \quad (4.23a)$$

$$\frac{d\tilde{\tau}}{d\ell} = -\tilde{g}^2. \quad (4.23b)$$

These can be easily integrated by multiplying Eqs. (4.23a) and (4.23b) by \tilde{g} and $\tilde{\tau}$, respectively, and taking the difference of the two resulting equations. The result is that near T_{c0} the flows are a family of hyperbolas

$$\tilde{g}^2 - \tilde{\tau}^2 = c, \quad (4.24)$$

labeled by a constant of integration

$$c = \left(\frac{\sqrt{2}p^2g}{K\Lambda^2} \right)^2 - \left(\frac{Tp^2}{4\pi K} - 2 \right)^2, \quad (4.25)$$

determined by the bare value of model parameters g and K . The resulting flows are illustrated in Fig. 4, showing three distinct regions of behavior. In the high-temperature region below the thick line ($c < 0$), pinning is irrelevant, and it therefore describes the rough phase, separated from the low-temperature smooth phase (the region above the thick line) by a critical line separatrix $\tilde{\tau} = \tilde{g}$. The latter therefore defines a true critical temperature given by

$$T_c = T_{c0} \left(1 + \frac{p^2g}{\sqrt{2}K\Lambda^2} \right), \quad (4.26)$$

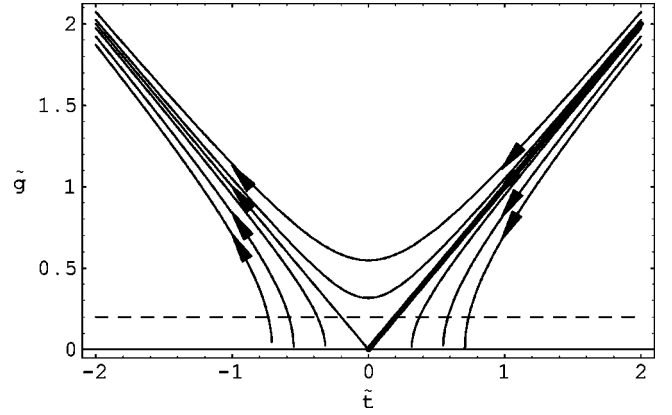


FIG. 4. Renormalization-group flow in the $(\tilde{\tau}, \tilde{g})$ plane. Temperature variation for an actual system occurs along the dashed line. On the high-temperature side of the separatrix $\tilde{\tau} = \tilde{g}$ (indicated as the thick line), the periodic pinning \tilde{g} renormalizes to zero and the interface is rough on long-length scales. Below T_c (to the left of the critical separatrix), the RG flow runs off to strong coupling \tilde{g} describing an interface that is smooth on long-length scales.

distinct from its $g \rightarrow 0$ limit of $T_{c0} = 8\pi K/p^2$. Changing T corresponds to the variation of the dimensionless bare parameters along the dashed horizontal line indicated in Fig. 4.

Above T_c , $\tilde{g}(\ell)$ flows to zero and

$$\tilde{\tau}_R \equiv \tilde{\tau}(\ell \rightarrow \infty) \quad (4.27a)$$

$$= \sqrt{|c|}, \quad (4.27b)$$

corresponding to the long-scale renormalized elastic constant

$$K_R \equiv K(\ell \rightarrow \infty) \quad (4.28a)$$

$$= K \frac{T}{T_{c0}} (1 + \sqrt{|c|}/2)^{-1}. \quad (4.28b)$$

It is comforting to find [using Eq. (4.25)] that K_R reduces to its bare value K at high temperatures. Using the fact that near, but above T_c ,

$$c = \tilde{g}^2 - (\tilde{\tau}_c + \tau)^2 \quad (4.29a)$$

$$\approx -2\tilde{\tau}_c\tau, \quad (4.29b)$$

with the true reduced temperature relative to the true (finite g) T_c given by

$$\tau \equiv \left(\frac{2T_c}{T_{c0}} \right) \frac{T - T_c}{T_c}, \quad (4.30)$$

and $\tilde{\tau}_c = \tilde{g} = 2(T_c/T_{c0} - 1)$, we find that in the limit $T \rightarrow T_c^+$

$$K_R(T) = K \frac{T_c}{T_{c0}} (1 - \sqrt{\tilde{g}} |T/T_c - 1|^{1/2}). \quad (4.31)$$

This leads at T_c to a renormalized value of the elastic constant $K_R(T_c^+)$ that is enhanced relative to the bare value K and with the universal ratio to T_c given by (Fig. 5)

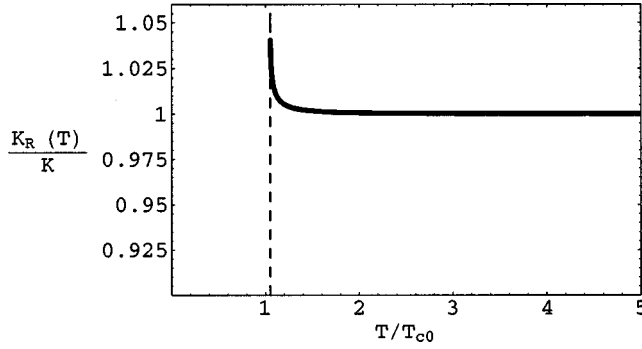


FIG. 5. Effective interface stiffness as a function of T/T_{c0} for $\tilde{g}=0.1$. In the smooth phase, K_R scales with the system size, and is effectively infinite. At $T=T_c^+$, K_R takes the value $K_R(T_c^+)=K(1+p^2g/\sqrt{2}K\Lambda^2)$ with a universal ratio $p^2/8\pi$ to the transition temperature T_c . Far above T_c , K_R goes to its bare value K . The dashed line indicates the location of T_c , which here is given by $T_c=1.05T_{c0}$.

$$\frac{K_R(T_c^+)}{T_c} = \frac{p^2}{8\pi}, \quad (4.32)$$

consistent with the analogous result first discovered in the context of the XY model,⁷¹ related to our problem by duality.^{41,72,73}

Below T_c , the relative pinning strength runs off to strong coupling and the interface is smooth on length scales longer than the correlation length that we calculate below. Because the RG flows are qualitatively very different near and away from the two separatrices $\tilde{g}=\pm\tilde{\tau}$, the value of this important length scale that enters the velocity-force characteristics depends crucially on the distance from T_c . In the critical region, defined by values of the bare parameters such that the weak-coupling (g) flow is near and roughly along either separatrix,

$$\tilde{g}(\ell) \approx \pm \tilde{\tau}(\ell), \quad (4.33a)$$

$$\approx \frac{\tilde{g}}{1 \pm \tilde{g}\ell}, \quad (4.33b)$$

it is easy to show that the RG “time” ℓ_* to reach strong coupling is given by

$$\ell_* \approx \frac{2}{\sqrt{c}} \quad (4.34a)$$

$$\approx \frac{2}{\sqrt{2\tilde{\tau}_c|\tau|}}. \quad (4.34b)$$

Consequently, the correlation length in this critical region is of familiar Kosterlitz-Thouless (KT) form⁷⁰

$$\xi_c \approx a e^{\ell_*} \quad (4.35a)$$

$$\approx a e^{\alpha|1-T/T_c|^{1/2}}, \quad (4.35b)$$

diverging extremely fast as $T \rightarrow T_c^-$, with $\alpha = \sqrt{2/\tilde{g}} = (T_c/T_{c0}-1)^{-1/2}$ a nonuniversal constant.

Outside this critical region, defined by $\tau < -1$, deep in the smooth phase, the flows are qualitatively different. At weak coupling, $gp^2 \ll K\Lambda^2$ (the only regime where the perturbative RG analysis is valid) because $\tilde{\tau}(\ell)$ grows weakly (additively),

$$\tilde{g}(\ell) \approx \tilde{g} e^{(2-\eta)\ell}, \quad (4.36)$$

grows exponentially fast, reaching strong coupling at the low- T correlation length $\xi_g \approx a e^{\ell_g}$ given by

$$\xi_g \approx \xi_0 (\xi_0 \Lambda)^{\eta/(2-\eta)} \quad (4.37a)$$

$$\approx \Lambda^{-1} (\Lambda \xi_0)^{2/(2-\eta)} \quad (4.37b)$$

$$\approx \Lambda^{-1} \left(\frac{K\Lambda}{p^2g} \right)^{1/(2-\eta)}. \quad (4.37c)$$

On scales longer than the roughness correlation length, the interface is smooth and is characterized by a strongly downward renormalized value of the pinning strength g_R determined by the value of *unrescaled* coupling $g(\ell = \ln(\xi\Lambda))$ at the scale of the correlation length. Near the transition

$$g_R \approx g(\Lambda\xi)^{-2} \ll g, \quad T \rightarrow T_c^- \quad (4.38a)$$

$$\approx g e^{-2\alpha|1-T/T_c|^{1/2}}. \quad (4.38b)$$

Deep in the smooth phase, for weak pinning, we instead find

$$g_R \approx g(\Lambda\xi)^{-\eta} \ll g, \quad T \ll T_c \quad (4.39a)$$

$$\sim g^{2/(2-\eta)}, \quad (4.39b)$$

which for weak g is also substantially reduced by thermal fluctuations.

For strong pinning, fluctuations are unimportant and the correlation length reduces to the substantially shorter strong-coupling value $\xi_0 = (K/gp^2)^{1/2}$ determined by the bare model parameters.

B. Analysis of the equilibrium dynamics

We now turn our attention to the equilibrium ($F=\lambda=0$) dynamics of the sine-Gordon interface, characterized by an additional model parameter, the friction coefficient γ , with the RG flow given by

$$\frac{d\gamma}{d\ell} = \frac{1}{8} \tilde{g}^2 \eta \gamma. \quad (4.40)$$

Combining this with the recursion relation, Eq. (4.18b), we find that the renormalized surface stiffness K_R and friction coefficient γ_R are related by

$$\gamma_R = \gamma \left(\frac{K_R}{K} \right)^{1/2}. \quad (4.41)$$

This together with the results of the preceding section, show that the macroscopic *linear* mobility γ_R^{-1} is finitely renor-

malized in the rough phase $T > T_c$ and displays a square-root cusp approach to $\gamma_R^{-1}(T_c^+) = \gamma^{-1}(T_{c0}/T_c)^{1/2}$ as $T \rightarrow T_c^+$,

$$\gamma_R^{-1}(T) \approx \gamma_R^{-1}(T_c^+) \left(1 + \frac{1}{2} \sqrt{\bar{g}} |T/T_c - 1|^{1/2} \right), \quad (4.42)$$

similar to the results of Petschek and Zippelius⁷⁴ for the renormalized diffusion coefficient of the XY model as $T \rightarrow T_{KT}^-$.

The effective friction coefficient $\gamma(\ell)$ at scale e^ℓ can be obtained by integrating the flow equation (4.40),

$$\gamma(\ell) = \gamma \exp \left[\frac{1}{8} \int_0^\ell d\ell' \bar{g}^2(\ell') \eta(\ell') \right]. \quad (4.43)$$

Since below T_c , at weak coupling, $\bar{g}^2(\ell) \eta(\ell)$ grows with ℓ , we find that the effective friction coefficient runs off to infinity as $\ell \rightarrow \infty$ suggesting a vanishing of the macroscopic linear mobility in the smooth phase. A more detailed analysis of the equilibrium weak-coupling flow equations for large ℓ gives

$$\gamma(\ell) \approx \gamma \begin{cases} \exp \left[\frac{|\tau| \ell}{4\alpha^2} \right], & T \rightarrow T_c^- \\ \exp \left[\frac{\eta \bar{g}^2 e^{2(2-\eta)\ell}}{16(2-\eta)} \right], & T \ll T_c. \end{cases} \quad (4.44)$$

Such diverging friction coefficient can be physically interpreted as activated creep dynamics over a pinning energy barrier that asymptotically grows with length scale, logarithmically for $T \rightarrow T_c^-$ and as a power law for $T \ll T_c$.

It is important to keep in mind that this growth of the friction coefficient $\gamma(\ell)$ found in Eq. (4.44) extends only up to the strong-coupling length scale $\xi = ae^{\ell^*}$ [ξ_c for $T \rightarrow T_c^-$, Eq. (4.35b), and ξ_g for $T \ll T_c$, Eq. (4.37c)], since it was derived based on a renormalization-group approach that is perturbative in \bar{g} . In Sec. V, we will look in more detail at the physics on scales longer than ξ , but we can already say at this point that (as we show in Sec. V) even in this strong-coupling regime the effective friction coefficient diverges. Consequently, we find that the interface linear (and in fact any order- n) mobility exhibits a nonuniversal jump discontinuity to zero across the roughening transition,^{48,49} as illustrated in Fig. 6.

V. NONEQUILIBRIUM DYNAMICS AND THE VELOCITY-FORCE CHARACTERISTICS

A. Weak-coupling regime

We now turn to the full nonequilibrium problem, with the aim of deriving the velocity-force characteristics of an interface driven through a weak periodic potential, going beyond the failing (for $T < T_c$) perturbative approach of Sec. III. As long as the pinning remains weak, the long-scale physics of the driven interface is contained in the renormalization-group equations, (4.21)–(4.26), which when rewritten in terms of the dimensionless variables \bar{g} , η , f , and the new KPZ coupling

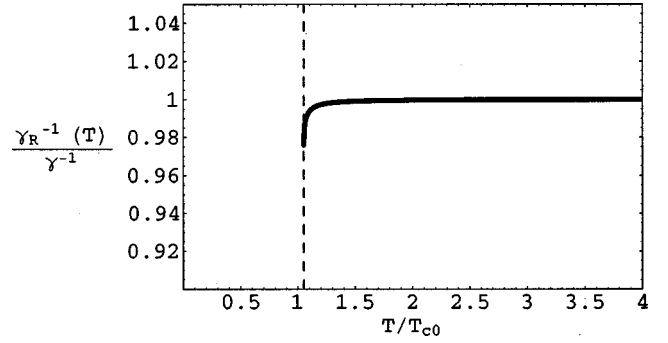


FIG. 6. Effective linear mobility γ_R^{-1} as a function of T/T_{c0} in equilibrium ($F=0$) for $\bar{g}=0.1$. Below the roughening temperature at T_c , the mobility vanishes and the interface is pinned. $\gamma_R^{-1}(T)$ shows a square-root cusp as $T \rightarrow T_c^+$, and goes to its bare value γ^{-1} for $T \gg T_c$. The dashed line indicates the location of T_c , which here is given by $T_c = 1.05T_{c0}$.

$$\tilde{\lambda} = \frac{\lambda}{pK} \quad (5.1)$$

are given by

$$\frac{d\gamma}{d\ell} = \frac{1}{8} \eta \bar{g}^2 \frac{1-f^2}{(1+f^2)^2} \gamma, \quad (5.2)$$

$$\frac{d\bar{g}}{d\ell} = (2-\eta)\bar{g}, \quad (5.3)$$

$$\frac{d\eta}{d\ell} = \frac{1}{2} \eta^2 \tilde{\lambda}^2 + \frac{1}{8} \eta^2 \bar{g}^2 \frac{-2+5f^2+3f^4}{(1+f^2)^3}, \quad (5.4)$$

$$\frac{d\tilde{\lambda}}{d\ell} = \frac{1}{8} \eta \bar{g}^2 \frac{f(f^2+5)}{(1+f^2)^3}, \quad (5.5)$$

$$\frac{df}{d\ell} = 2f + \frac{1}{2} \eta \tilde{\lambda} - \frac{1}{8} \eta \bar{g}^2 \frac{f(3-f^2)}{(1+f^2)^3}. \quad (5.6)$$

The most striking effect of nonequilibrium dynamics is the breakdown of the FDT and as a result a nontrivial upward renormalization (flow) of the effective “temperature” $T(\ell)$ driven by the external force and the KPZ nonlinearity, reminiscent of nonequilibrium “heating” in randomly pinned systems.^{75,5-7} Consequently, even for $T < T_c$, for sufficiently strong drive the parameter $2-\eta(\ell)$ determining the long-scale behavior of the periodic potential is driven negative, leading to the irrelevance of the pinning potential. Hence, as discussed in the Introduction, a finite external drive removes the qualitative distinction between the rough and smooth phases and therefore rounds the roughening transition.^{48,49,51,53}

Here, we instead focus on the creep regime, where these particular nonequilibrium effects are unimportant. In this weak-driving creep regime, we can ignore the KPZ nonlinearity and the most important role of F , as can be clearly seen even at the level of perturbation theory, Eq. (3.5), and from the equation of motion, is to introduce a new length

scale $\xi_F \sim 1/\sqrt{F}$ defined in Eq. (3.24). Beyond this nonequilibrium length scale, the effects of the pinning potential and its ability to renormalize $\gamma(\ell)$ and $K(\ell)$ are suppressed, as it is averaged away on scales longer than ξ_F (see, for example, the RG flow equations above and analysis below). Hence, for weak external drive F , the effective values of friction and interface stiffness parameters are given by $\gamma(\ell_F)$ and $K(\ell_F)$ renormalized by Gaussian equilibrium fluctuations up to length scale $\xi_F = e^{\ell_F}$. This therefore translates the strong ℓ dependence of $\gamma(\ell)$ into strong F dependence of the macroscopic mobility $\gamma^{-1}(F)$. Substituting ξ_F , Eq. (3.24), inside our equilibrium flow, Eqs. (4.44), and using

$$v(F) = F/\gamma(\ell_F), \quad (5.7)$$

we immediately obtain the velocity-force characteristics, Eq. (1.2), quoted in the Introduction.

This prediction for $v(F)$, Eq. (1.2), applies as long as the relevant F probes length scales ξ_F on which the equilibrium *weak-coupling* flow equations remain valid. As discussed in the preceding section, these flows in fact break down due to strong-coupling effects (with g itself cutting off thermal Gaussian fluctuations) for length scales greater than ξ , Eqs. (4.35b) and (4.37c). Hence, our predictions for $v(F)$, Eq. (1.2), remain valid only as long as $\xi_F < \xi$ (i.e., it is the external force and not the periodic potential itself that cuts off the Gaussian fluctuations), which translates into the condition $F > F_*$, with the crossover force F_* given by Eq. (1.1) and in agreement with perturbation theory.

To see this weak-coupling phenomenology emerge directly from our full nonequilibrium flow equations, Eqs. (5.2)–(5.6), we integrate these equations, with $\lambda=0$ and ignoring the nonequilibrium flow of $T(\ell)$ (a valid approximation in the $F \rightarrow 0$ limit). We find for the renormalized friction coefficient the following intermediate result:

$$\gamma_R(f) = \gamma \exp \left[\frac{1}{8} \int_0^\infty d\ell \eta(\ell) \tilde{g}^2(\ell) \frac{1-f^2(\ell)}{[1+f^2(\ell)]^2} \right]. \quad (5.8)$$

Since at low drive and weak coupling, well below T_c , $\eta(\ell)$, $K(\ell)$, and $T(\ell)$ grow slowly and $f(\ell)$ and $\tilde{g}(\ell)$ grow strongly according to

$$\tilde{g}(\ell) = \tilde{g} e^{(2-\eta)\ell}, \quad (5.9a)$$

$$f(\ell) \approx f e^{2\ell}, \quad (5.9b)$$

it is quite clear from Eq. (5.8) that as long as the weak-coupling flows remain valid, in the smooth phase the flows are automatically cut off when $f(\ell)$ gets to be >1 leading to ℓ_F discussed above.

Substituting Eqs. (5.9) into the expression of $\gamma_R(f)$, Eq. (5.8), and integrating the resulting expression, we find

$$\gamma_R(f) = \gamma \exp \left[\frac{1}{8} \eta \tilde{g}^2 A \left(-\frac{\tilde{\tau}}{2}, f \right) \right], \quad (5.10)$$

with $-\tilde{\tau}/2 = (2-\eta)/2 = (1-T/T_{c0})$, and $A(x,f)$ is the function given by

$$A(x,f) = \frac{1}{2f^4} \left[\frac{1}{2(2-x)} {}_2F_1(2,2-x,3-x,-f^{-2}) - 2f^2(1-x) {}_2F_1 \left(2,1-x,2-x,-\frac{1}{f^2} \right) \right], \quad (5.11)$$

where ${}_2F_1$ denotes a hypergeometric function.⁷⁶ When $T < T_c$ [i.e., $(-\tilde{\tau}) > 0$], taking the limit of the function $A(-\tilde{\tau}/2,f)$ of Eq. (5.10) when $f \rightarrow 0$ leads to the following expression for the long-scale inverse of nonlinear mobility γ_R :

$$\gamma_R(f) = \gamma \exp[(F_*/F)^{2(1-T/T_c)}], \quad (5.12)$$

with

$$F_*(\tilde{g},T) \approx \frac{2K\Lambda^2}{p} \left(\frac{\eta \tilde{g}^2}{16(2-\eta)} \right)^{1/2(1-T/T_c)}, \quad (5.13)$$

in full agreement with earlier more qualitative discussion of the velocity-force characteristics in the intermediate regime of forces $F > F_*$, and F_* consistent with the perturbative result (3.22) for $\tilde{g} \ll 1$ (Fig. 7).

As F is lowered below F_* , eventually the saturation of $\gamma(\ell)$ breaks down and the flow behavior changes dramatically as strong-coupling length scales (at which our weak-coupling RG solution is invalid) are probed. Studying the point at which this happens as a function of model parameters, allows us to extract the crossover value of F_* , which we plot in Fig. 8. We find that there is a qualitative agreement between the analytical prediction for f_* , Eq. (3.22), and our numerical analysis.

B. Strong-coupling regime

The weak-coupling behavior found in the preceding section only extends up to the scale ξ , Eqs. (4.35b) and (4.37c). Beyond this strong-coupling length, in the equilibrium model, the growth of $\tilde{g}(\ell)$ and $\gamma(\ell)$ is cut off by the pinning potential, and an approach nonperturbative in \tilde{g} , where pinning is treated on equal footing with the elastic energy, is required. In this strong-coupling regime Gaussian interface fluctuations, considered so far, are strongly suppressed by the pinning barrier that scales like L^2 relative to the elastic energy.

Instead, at low temperature the fluctuations are dominated by nontrivial saddle-point solutions (solitons) of H , Eq. (2.1), with model parameters, K_R , g_R , γ_R renormalized by Gaussian fluctuations on weak-coupling scales $L < \xi$. The dominant soliton excitation, illustrated in projection in Fig. 9, corresponds to a circular patch of radius $R > \xi$ of a nearly flat interface moving over to a neighboring minimum of the periodic potential, with an energy cost that clearly grows linearly with R ,

$$E_{\text{soliton}}(R) \approx p g_R \xi R, \quad (5.14)$$

where g_R [Eqs. (4.38) and (4.39)] and ξ [Eqs. (4.35b) and (4.37c)] strongly depend on the proximity to T_c . At zero drive, the barrier to such solitonic motion simply diverges

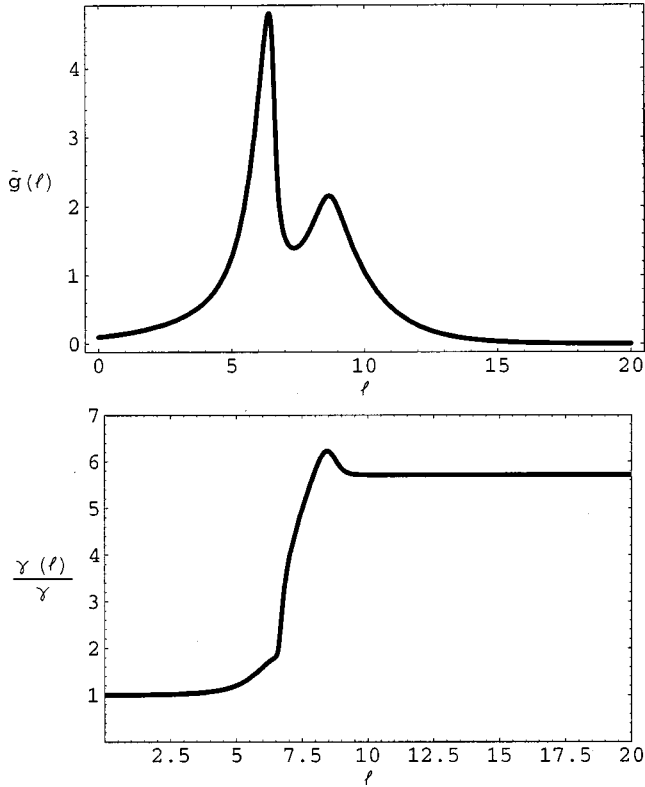


FIG. 7. Behavior of the pinning strength g (top) and of the friction coefficient $\gamma(\ell)$ (bottom) with length scale ℓ for $\bar{g}=0.1$, $T \approx 0.8T_c$, and $f \approx 1.7374 \times 10^{-5}$. Here $f_* \approx 1.7373 \times 10^{-5}$.

and linear mobility vanishes identically. A velocity-force characteristic in the weak drive $F < F_*$ (i.e., $\xi < \xi_F$) regime can be analyzed via scaling nucleation theory.⁴⁸ In this creep regime, the interface is in near metastable equilibrium with F introducing a contribution

$$E_F(R) \approx -F \pi R^2 d \quad (5.15)$$

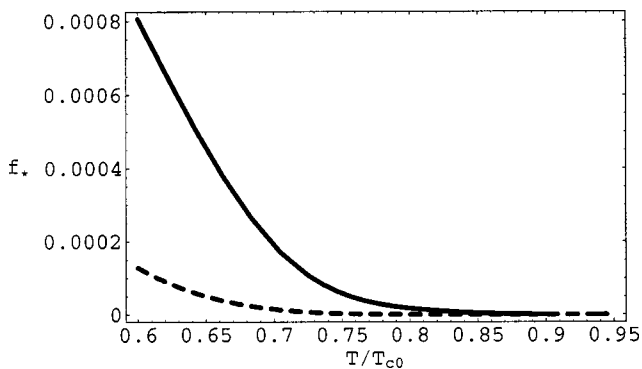


FIG. 8. Characteristic force $f_*(T)$ as obtained from the numerical solution of the dynamic RG recursion relations (solid line) and from the perturbative estimate of Eq. (3.22), (dashed line), for $\bar{g} = 0.1$. The curve $f_*(T)$ delimits two very different physical regimes. Above this curve, the interface moves with uniform velocity. On the other hand, for $f < f_*(T)$, the interface moves through the nucleation of soliton excitations.

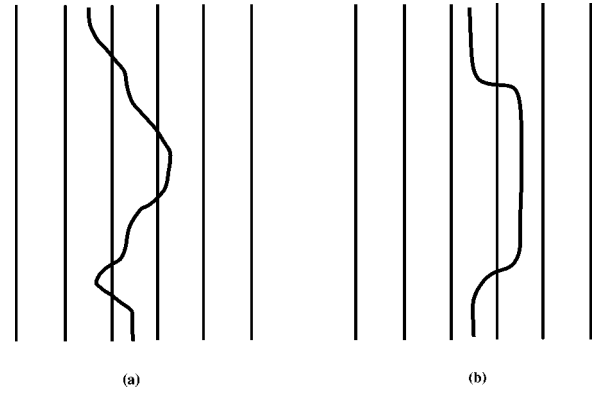


FIG. 9. Schematic representation of the motion of a driven interface past the periodic pinning potential. (a) When $T > T_c$, or $T < T_c$ and $f > f_*$, the large fluctuations of the interface wash out the pinning potential on large length scales and the interface moves with a uniform velocity. (b) On the other hand, for $T < T_c$ and $f < f_*$, the fluctuations of the interface are small; as a result, most of the interface is pinned at a given minimum of the pinning potential, and motion from one minimum to the next takes place through soliton excitations.

to the effective free energy. Balancing $E_F(R)$ against the soliton energy $E_{\text{soliton}}(R)$, we find that solitons of size larger than a critical radius

$$R_c \approx \left(\frac{p g_R \xi}{2 \pi d} \right) \frac{1}{F} \quad (5.16)$$

are unstable. In the $F \rightarrow 0$ limit, thermal activation rate of solitons of size $R_c \sim 1/F$ is quite clearly the limiting step for interface creep motion. We therefore find that the weak-coupling velocity-force characteristics, Eq. (1.2), cross over, for $F < F_*$, to that given by Eq. (1.3) in the Introduction, with

$$F_0 \approx \frac{(p g_R \xi)^2}{4 \pi d}. \quad (5.17)$$

For vanishing temperature and strong bare pinning potential, our asymptotic (for $F < F_*$) result for $v(F)$ reduces to that found in Refs. 48 and 4. However, at large $T < T_c$ and weak bare pinning g , we predict a strong thermal renormalization of the characteristic pinning energy

$$p^2 g^2 a^2 \rightarrow p^2 g_R^2 \xi^2 \quad (5.18)$$

by thermal fluctuations on scales smaller than ξ .

VI. DISCUSSION AND CONCLUSIONS

In this paper, we have studied the creep dynamics of a two-dimensional interface driven through a periodic potential. Using dynamic renormalization-group methods and matching to strong coupling, we have calculated the velocity-force characteristics across the interface roughening transition. Consistent with previous studies, we find a qualitative change across the transition in the weak-drive velocity-force characteristics, with Ohmic transport for $T > T_c$ and a jump discontinuity in mobility across the transi-

tion. For $T < T_c$, in the asymptotic creep regime $F \ll F_*(g, T)$ and for strong bare coupling, where transport is via soliton activation at all scales, we recover previously found results for the velocity-force characteristics $v(F)$. However, for weak bare coupling and strong-thermal fluctuations, we predict an intermediate drive $F > F_*(g, T)$ nonlinear regime with a continuously varying (with T) exponent, which asymptotically crosses over to the strong-coupling result with strongly thermally renormalized characteristic pinning barrier. Unfortunately, because the characteristic force $F_*(g, T)$ that delineates between the intermediate drive regime and the strong-coupling regime coincides with the force marking the breakdown of the perturbative high-velocity expansion, we expect it to be difficult to observe this intermediate drive regime.

The physical picture which emerges from the present study complements previously made predictions⁴ which were based on a more elementary perturbative approach, as well as known results for the mobility^{48,49} at zero external drive. On the experimental side, the above picture may shed some light on experiments such as those of Wolf *et al.*,³⁴ who found that the growth velocity v of a surface of crystalline helium 4 is strongly reduced at T_c from an Ohmic behavior $v \sim F$ for $T > T_c$ to an extremely slow growth rate for $T < T_c$, a result which is usually explained in terms of an onset of creep motion via solitonlike excitations.⁴⁸

An interesting and experimentally relevant generalization of our results is a study of creep dynamics of a two-dimensional solid, driven through a one- or two-dimensional periodic potential, with applications to driven 2D colloidal crystals and vortices in superconducting films. Despite considerably different geometry, in equilibrium these systems display a pinned-to-floating solid transition closely related to the roughening transition of 2D interfaces. However, different interesting ingredients arise. Some of the most important ones are the nonequilibrium convective-like terms,^{77,17,6} vector phonon displacement and concomitant possible importance of dislocations. Combined with the considerably interesting behavior of the scalar sine-Gordon model studied here, we expect these to lead to even richer phenomenology. We expect that studies of these will shed considerable light on numerous experiments and simulations.⁷⁸

ACKNOWLEDGMENTS

L.R. thanks Harvard Physics Department for hospitality and Daniel Fisher and John Toner for discussions. We acknowledge financial support by the National Science Foundation through Grant No. DMR-9625111, the University of Colorado (L.R.), and by the A. P. Sloan, and David and Lucile Packard Foundations.

APPENDIX: STATIC MOMENTUM-SHELL RENORMALIZATION GROUP

In this appendix, we present technical details on the derivation of the renormalization-group recursion relations for the driven sine-Gordon model in 2+1 dimensions. For completeness, we shall begin in Sec. 2 of this appendix by show-

ing how the standard momentum shell⁷⁹ RG with hard cutoff^{80,81} can be applied to the static version of this problem before deriving the full dynamic equations at nonzero external drive in Sec. 2.

1. Static RG

We decompose the field $h(\mathbf{r})$ in the Hamiltonian (2.1) into high and low wave-vector components

$$h(\mathbf{r}) = h^<(\mathbf{r}) + h^>(\mathbf{r}) \quad (\text{A1})$$

such that

$$h^<(\mathbf{r}) = \int_{\mathbf{q}}^< h(\mathbf{q}) e^{i\mathbf{q}\cdot\mathbf{r}}, \quad (\text{A2})$$

$$h^>(\mathbf{r}) = \int_{\mathbf{q}}^> h(\mathbf{q}) e^{i\mathbf{q}\cdot\mathbf{r}}, \quad (\text{A3})$$

where $\int_{\mathbf{q}}^< \equiv \int_0^{\Lambda/b} d\mathbf{q}/(2\pi)^2$ and $\int_{\mathbf{q}}^> \equiv \int_{\Lambda/b}^{\Lambda} d\mathbf{q}/(2\pi)^2$ denote integration in momentum space over the ranges $0 < |\mathbf{q}| < \Lambda/b$ and $\Lambda/b < |\mathbf{q}| < \Lambda$, respectively. In terms of these high- and low-momentum fields, the equilibrium Hamiltonian $H_0[h] = \frac{1}{2} \int d\mathbf{r} K(\nabla h)^2$ can be written as the sum

$$H_0[h] = H_0[h^<] + H_0[h^>].$$

We now want to integrate over the fast component $h^>(\mathbf{r})$. To this end, we rewrite the partition function $Z = \int [dh] \exp(-\beta H)$ in the form (here $\beta = 1/T$ is the inverse temperature)

$$\begin{aligned} Z &= \int [dh^<][dh^>] e^{-\beta H_0[h^<] - \beta H_0[h^>] - \beta H_1[h^< + h^>]} \\ &= \int [dh^<] e^{-\beta H_0[h^<]} \int [dh^>] e^{-\beta H_0[h^>] - \beta H_1[h^< + h^>]} \\ &= \int [dh^<] e^{-\beta H_0[h^<] + \beta \ln Z_0^>} \langle e^{-\beta H_1[h^< + h^>]} \rangle_{0>}, \quad (\text{A4}) \end{aligned}$$

where $Z_0^> = \int [dh^>] \exp(-\beta H_0[h^>])$, and where the subscript $(0>)$ means that the average with respect to $h^>$ is performed with statistical weight $\exp(-\beta H_0[h^>])/Z_0^>$. The term between angular brackets in Eq. (A4) is then approximated by a cumulant expansion

$$\langle e^{-\beta H_1[h^< + h^>]} \rangle_{0>} = 1 - \frac{\langle H_1 \rangle_{0>}}{T} + \frac{1}{2T^2} \langle H_1^2 \rangle_{0>}^c + \dots, \quad (\text{A5})$$

where $\langle H_1^2 \rangle_{0>}^c$ denotes the second cumulant $\langle (H_1^2 - \langle H_1 \rangle^2) \rangle_{0>}$. When reexponentiated, Eq. (A5) leads to the result

$$\langle e^{-\beta H_1[h^< + h^>]} \rangle_{0>} = e^{-\beta H_{eff}}, \quad (\text{A6})$$

with the effective Hamiltonian

$$H_{eff} = \langle H_1 \rangle_{0>} - \frac{1}{2T} \langle H_1^2 \rangle_{0>}^c + \dots \quad (\text{A7})$$

The averages in Eq. (A5) can be easily evaluated, with the results^{44,48}

$$\langle H_1 \rangle_{0>} = -g e^{-(1/2)p^2 G^>(0)} \int d\mathbf{r} \cos[ph^<(\mathbf{r})], \quad (\text{A8})$$

$$\begin{aligned} \langle H_1^2 \rangle_{0>}^c &= \frac{1}{2} g^2 e^{-p^2 G^>(0)} \int d\mathbf{r} d\mathbf{r}' [e^{p^2 G^>(\mathbf{r}-\mathbf{r}')} - 1] \\ &\quad \times (\cos\{p[h^<(\mathbf{r}) + h^<(\mathbf{r}')] \} \\ &\quad + \cos\{p[h^<(\mathbf{r}) - h^<(\mathbf{r}')] \}), \end{aligned} \quad (\text{A9})$$

where $G^>(\mathbf{r}-\mathbf{r}') = \langle h^>(\mathbf{r})h^>(\mathbf{r}') \rangle_{0>}$ is the elastic propagator for fast fields (here J_0 is the zeroth-order Bessel function)

$$G^>(\mathbf{r}-\mathbf{r}') = T \int_{\mathbf{q}} \frac{e^{i\mathbf{q}\cdot(\mathbf{r}-\mathbf{r}')}}{Kq^2} = \frac{T d\ell}{2\pi K} J_0(\Lambda|\mathbf{r}-\mathbf{r}'|). \quad (\text{A10})$$

Given that $G^>(0) = Td\ell/2\pi K$, we see that the first-order cumulant (A8), after the rescalings (A18) and (A19), leads straightforwardly to the recursion relation (4.18a) for the pinning strength g . On the other hand, since the ‘‘kernel’’

$$\mathcal{K}(\mathbf{r}) = [e^{p^2 G^>(\mathbf{r})} - 1] \quad (\text{A11})$$

takes appreciable values only for small values of its argument, we see that the first term inside the integral in Eq. (A9) will contribute higher harmonic terms ($\sim \cos[2ph^<(\mathbf{r})]$) to the effective Hamiltonian, and hence we shall discard this term as irrelevant. In the second term, we shall make the approximation

$$\begin{aligned} \cos\{p[h^<(\mathbf{r}) - h^<(\mathbf{r}')] \} \\ \simeq 1 - \frac{1}{2} p^2 [h^<(\mathbf{r}) - h^<(\mathbf{r}')]^2 \\ \simeq 1 - \frac{1}{2} p^2 (\mathbf{r}-\mathbf{r}')_\alpha (\mathbf{r}-\mathbf{r}')_\beta \partial_\alpha h^<(\mathbf{r}) \partial_\beta h^<(\mathbf{r}'), \end{aligned} \quad (\text{A12})$$

where, in going from the first to the second line, we made use of the Taylor expansion

$$h^<(\mathbf{r}) - h^<(\mathbf{r}') \simeq (\mathbf{r}-\mathbf{r}')_\alpha \partial_\alpha h^<(\mathbf{r}).$$

Inserting Eq. (A12) back into Eq. (A9), we obtain the following approximation to the second cumulant (we here use the symbol \equiv to indicate that we retain only the term correcting the stiffness K):

$$\begin{aligned} \langle H_1^2 \rangle_{0>}^c &\equiv -\frac{1}{8} p^2 g^2 e^{-p^2 G^>(0)} \int d\mathbf{r} [\nabla h^<(\mathbf{r})]^2 \\ &\quad \times \int d\mathbf{r}' (\mathbf{r}-\mathbf{r}')^2 \mathcal{K}(\mathbf{r}-\mathbf{r}'). \end{aligned} \quad (\text{A13})$$

Since $G^>\propto d\ell = \ln b$, we can expand the exponential in a Taylor series in $G^>$,

$$e^{p^2 G^>(\mathbf{r}-\mathbf{r}')} - 1 \simeq p^2 G^>(\mathbf{r}-\mathbf{r}') + \frac{1}{2!} p^4 [G^>(\mathbf{r}-\mathbf{r}')]^2. \quad (\text{A14})$$

Now, the renormalization of K involves the integral

$$\int d\mathbf{r} r^2 \mathcal{K}(\mathbf{r}) = \int d\mathbf{r} r^2 [e^{p^2 G^>(\mathbf{r})} - 1]. \quad (\text{A15})$$

Inserting the expansion (A14) into this last expression, the first term gives a contribution⁸²

$$\int d\mathbf{r} r^2 G^>(\mathbf{r}) = -\nabla_{\mathbf{q}}^2 G^>(\mathbf{q})|_{\mathbf{q}=0} \quad (\text{A16})$$

which vanishes identically, since $G^>(\mathbf{q})$ has support only on the shell $\Lambda/b < q < \Lambda$. The second term gives

$$\int d\mathbf{r} r^2 \mathcal{K}(\mathbf{r}) = \frac{1}{4} p^4 \int d\mathbf{r} r^2 [G^>(\mathbf{r})]^2 = \frac{T^2 p^4 \ln b}{\pi K^2 \Lambda^4}. \quad (\text{A17})$$

Thus, we obtain for the second cumulant (A13) the following expression:

$$-\frac{\langle H_1^2 \rangle_{0>}^c}{2T} \equiv \frac{T p^6 g^2 d\ell}{8\pi K^2 \Lambda^4} \int d\mathbf{r} \frac{1}{2} [\nabla h^<(\mathbf{r})]^2.$$

We now perform the following rescalings:

$$\mathbf{r} = e^\ell \mathbf{r}', \quad (\text{A18})$$

$$h^<(\mathbf{r}) = e^{\chi\ell} h^<(\mathbf{r}'), \quad (\text{A19})$$

so as to restore the ultraviolet cutoff back to Λ . Because the pinning potential is a periodic function, it is convenient (although not necessary) to set the arbitrary field dimension χ to zero, thereby preserving the period $2\pi/p$ of the original problem under RG transformations. Under such a transformation, the resulting effective Hamiltonian can be cast into its original form with effective ℓ -dependent parameters $K(\ell)$ and $g(\ell)$ such that

$$g(\ell) = g e^{(2-Tp^2/4\pi K)\ell}, \quad (\text{A20a})$$

$$K(\ell) = K + \frac{T p^6 g^2}{8\pi K^2 \Lambda^4} d\ell, \quad (\text{A20b})$$

or, in differential form

$$\frac{dg}{d\ell} = \left(2 - \frac{T p^2}{4\pi K}\right) g, \quad (\text{A21a})$$

$$\frac{dK}{d\ell} = \frac{T p^6 g^2}{8\pi K^2 \Lambda^4}. \quad (\text{A21b})$$

2. Dynamic RG

We now turn our attention to the derivation of the dynamic RG flow equations (4.16a)–(4.16f) for the driven sine-Gordon model. As we did in the static case, we define the following low- and high-momentum components $h^<(\mathbf{r}, t)$ and $h^>(\mathbf{r}, t)$:

$$u^<(\mathbf{r}, t) = \int_{\mathbf{q}, \omega}^< h(\mathbf{q}, \omega) e^{i(\mathbf{q} \cdot \mathbf{r} - \omega t)}, \quad (\text{A22})$$

$$u^>(\mathbf{r}, t) = \int_{\mathbf{q}, \omega}^> h(\mathbf{q}, \omega) e^{i(\mathbf{q} \cdot \mathbf{r} - \omega t)}, \quad (\text{A23})$$

where, here and in what follows, $\int_{\mathbf{q}, \omega}$ on integrals stands for

$$\int \frac{d^d \mathbf{q}}{(2\pi)^d} \frac{d\omega}{2\pi},$$

and the superscripts $>$ and $<$ indicate integration over the high- ($\Lambda/b < q < \Lambda$) and low- ($0 < q < \Lambda$) momentum regions, respectively. Using the fact that $u(\mathbf{q}, \omega) = u^<(\mathbf{q}, \omega) + u^>(\mathbf{q}, \omega)$, it is not difficult to verify that the free part S_0 of the action decomposes into two diagonal pieces $S_0^<$ and $S_0^>$ depending only on $u^<(\mathbf{q}, \omega)$ and $u^>(\mathbf{q}, \omega)$, respectively,

$$S_0[u, \tilde{u}] = S_0[u^<, \tilde{u}^<] + S_0[u^>, \tilde{u}^>]. \quad (\text{A24})$$

As we did in the static RG, in order to be able to integrate out the fast component of the field $u(\mathbf{r}, t)$, we rewrite the generating functional \mathcal{Z} in the form

$$\begin{aligned} \mathcal{Z} = & \int [du^<][d\tilde{u}^<] \\ & \times e^{-S_0[u^<, \tilde{u}^<] + \ln \mathcal{Z}_0^> \langle e^{-S_1[u^< + u^>, u^< + u^>]} \rangle_0}, \end{aligned}$$

where $\mathcal{Z}_0^> = \int [du^>][d\tilde{u}^>] \exp(-S_0[u^>, \tilde{u}^>])$, and where $\langle \cdots \rangle_0^>$ denotes statistical averaging with statistical weight $e^{-S_0[u^>, \tilde{u}^>]}$. The perturbative correction to the dynamic action can therefore be expressed in terms of a cumulant expansion

$$\langle e^{-S_1} \rangle_{0>} = 1 - \langle S_1 \rangle_{0>} + \frac{1}{2} \langle S_1^2 \rangle_{0>} + \cdots \quad (\text{A25})$$

Reexponentiation of this expansion allows us to define the effective action

$$S_{eff}[u, \tilde{u}] = S_0 + \langle S_1 \rangle_{0>} - \frac{1}{2} \langle [S_1^2 - (\langle S_1 \rangle_{0>}^2)] \rangle_{0>} + \cdots, \quad (\text{A26})$$

from which we can derive dynamic RG flows for the parameters of the original equation of motion. This procedure, to first order in the pinning strength g , has already been shown in the text. Here we are therefore only going to consider the second-order correction to the original action S . In fact, it turns out⁴⁹ that the only perturbative corrections to S to second order in perturbation theory come from the cumulants $-\frac{1}{2} \langle S_g^2 \rangle_{0>}$ and $-\frac{1}{2} \langle S_\lambda^2 \rangle_{0>}$, i.e., we need not consider the cross term $-\langle S_g S_\lambda \rangle_{0>}$ which does not provide any perturbative corrections to the action. In the following, we shall only show how we compute the perturbative corrections arising from the sine-Gordon perturbation $-\frac{1}{2} \langle S_g^2 \rangle_{0>}$, the unique term arising from $-\frac{1}{2} \langle S_\lambda^2 \rangle_{0>}$,

$$\Delta S_\lambda(\gamma T) = \int d\mathbf{r} dt \tilde{u}_<^2(\mathbf{r}, t) \left[\frac{T\lambda^2 d\ell}{8\pi K^3} \right], \quad (\text{A27})$$

having been repeatedly derived in the literature.^{51,83,49} Taking the Gaussian averages in Eq. (A25) leads to the following expression of the second cumulant $\Delta S_g[\tilde{u}, u] = -\frac{1}{2} \langle S_g^2 \rangle_{0>}^c$:

$$\begin{aligned} \Delta S_g[\tilde{u}^< u] = & -\frac{1}{2} p^2 g^2 \int d\mathbf{r} dt \int d\mathbf{r}' dt' \tilde{u}^<(\mathbf{r}, t) \tilde{u}^<(\mathbf{r}', t') \\ & \times \tilde{\mathcal{K}}(\mathbf{r} - \mathbf{r}', t - t') \\ & \times \cos \left[p[u^<(\mathbf{r}, t) - u^<(\mathbf{r}', t')] + \frac{pF}{\gamma}(t - t') \right] \\ & - \frac{1}{2} p^3 g^2 \int d\mathbf{r} dt \int d\mathbf{r}' dt' i \tilde{u}^<(\mathbf{r}, t) \\ & \times \mathcal{K}(\mathbf{r} - \mathbf{r}', t - t') \\ & \times \sin \left[p[u^<(\mathbf{r}, t) - u^<(\mathbf{r}', t')] + \frac{pF}{\gamma}(t - t') \right]. \end{aligned} \quad (\text{A28})$$

Here the dynamic kernels $\tilde{\mathcal{K}}(\mathbf{r}, t)$ and $\mathcal{K}(\mathbf{r}, t)$ are given by

$$\tilde{\mathcal{K}}(\mathbf{r}, t) = \frac{1}{2} \{ 1 - \cosh[p^2 G_0^>(\mathbf{r}, t)] \} - \sinh[p^2 G_0^>(\mathbf{r}, t)], \quad (\text{A29})$$

$$\mathcal{K}(\mathbf{r}, t) = e^{-(1/2) p^2 C_0^>(\mathbf{r}, t)} R_0^>(\mathbf{r}, t), \quad (\text{A30})$$

where $R_0^>(\mathbf{r}, t) = \int_{\mathbf{q}, \omega}^> e^{-i(\mathbf{q} \cdot \mathbf{r} - \omega t)} / (i\gamma\omega + Kq^2)$ and $C_0^>(\mathbf{r}, t) = \langle [u^>(\mathbf{r}, t) - u^>(\mathbf{0}, 0)]^2 \rangle$ are the response and correlation functions, respectively, and where the correlator $G_0^>(\mathbf{r}, t) = \langle u^>(\mathbf{r}, t) u^>(\mathbf{0}, 0) \rangle_{0>}$ is given by

$$G_0^>(\mathbf{r}, t) = 2\gamma T \int_{\mathbf{q}, \omega} \frac{\cos[\mathbf{q} \cdot \mathbf{r} - \omega t]}{\gamma^2 \omega^2 + K^2 q^4} \quad (\text{A31})$$

We now decompose the sine and cosine in the integrand on the rhs of Eq. (A28) according to

$$\begin{aligned} & \cos \left[p(u_< - u'_<) + \frac{pF}{\gamma}(t - t') \right] \\ & = \sin[p(u_< - u'_<)] \cos \left[\frac{pF}{\gamma}(t - t') \right] \\ & \quad + \cos[p(u_< - u'_<)] \sin \left[\frac{pF}{\gamma}(t - t') \right], \end{aligned} \quad (\text{A32a})$$

$$\begin{aligned} & \sin\left[p(u_{<} - u'_{<}) + \frac{pF}{\gamma}(t-t')\right] \\ &= \sin[p(u_{<} - u'_{<})] \cos\left[\frac{pF}{\gamma}(t-t')\right] \\ &+ \cos[p(u_{<} - u'_{<})] \sin\left[\frac{pF}{\gamma}(t-t')\right]. \end{aligned} \quad (\text{A32b})$$

The kernels $\tilde{\mathcal{K}}(\mathbf{r}-\mathbf{r}', t-t')$ and $\mathcal{K}(\mathbf{r}-\mathbf{r}', t-t')$ being short ranged both in space and time, we see that the major contribution to the action (A28) comes from the regions $\mathbf{r} \approx \mathbf{r}'$ and $t \approx t'$ where $[u^<(\mathbf{r}, t) - u^<(\mathbf{r}', t')]$ is small. We therefore shall approximate

$$\sin\{p[u^<(\mathbf{r}, t) - u^<(\mathbf{r}', t')]\} \approx p[u^<(\mathbf{r}, t) - u^<(\mathbf{r}', t')], \quad (\text{A33})$$

$$\begin{aligned} & \cos\{p[u^<(\mathbf{r}, t) - u^<(\mathbf{r}', t')]\} \\ & \approx 1 - \frac{1}{2} p^2 [u^<(\mathbf{r}, t) - u^<(\mathbf{r}', t')]^2, \end{aligned} \quad (\text{A34})$$

and

$$\begin{aligned} u^<(\mathbf{r}, t) - u^<(\mathbf{r}', t') &= (t-t') \partial_t u^< + (\mathbf{r}-\mathbf{r}')_\alpha \partial_\alpha u^< \\ &+ \frac{1}{2} (\mathbf{r}-\mathbf{r}')_\alpha (\mathbf{r}-\mathbf{r}')_\beta \partial_\alpha \partial_\beta u^<, \end{aligned} \quad (\text{A35})$$

upon which we obtain the following expression for the second cumulant $-\frac{1}{2} \langle S_1^2 \rangle_{0>}^c$:

$$\begin{aligned} \Delta S[\tilde{u}, u] &= -\frac{1}{2} \langle S^2 \rangle_{0>}^c [\tilde{u}, u] \\ &= \Delta S(\gamma T) + \Delta S(\gamma) + \Delta S(K) + \Delta S(\lambda) + \Delta S(F), \end{aligned} \quad (\text{A36})$$

where

$$\begin{aligned} \Delta S(\gamma T) &= \Delta S_\lambda(\gamma T) + \frac{1}{2} p^2 g^2 \int d\mathbf{r} dt \tilde{u}^<(\mathbf{r}, t) \tilde{u}^<(\mathbf{r}, t) \\ &\times \int d\mathbf{r}' dt' \tilde{\mathcal{K}}(\mathbf{r}-\mathbf{r}', t-t') \cos\left[\frac{pF}{\gamma}(t-t')\right], \end{aligned} \quad (\text{A37a})$$

$$\begin{aligned} \Delta S(\gamma) &= \frac{1}{2} p^4 g^2 \int d\mathbf{r} dt i \tilde{u}^<(\mathbf{r}, t) [\partial_t u^<(\mathbf{r}, t)] \\ &\times \int d\mathbf{r}' dt' (t-t') \mathcal{K}(\mathbf{r}-\mathbf{r}', t-t') \\ &\times \cos\left[\frac{pF}{\gamma}(t-t')\right], \end{aligned} \quad (\text{A37b})$$

$$\begin{aligned} \Delta S(K) &= \frac{1}{4} p^4 g^2 \int d\mathbf{r} dt i \tilde{u}^<(\mathbf{r}, t) [-\nabla^2 u^<(\mathbf{r}, t)] \\ &\times \int d\mathbf{r}' dt' (\mathbf{r}-\mathbf{r}')^2 \mathcal{K}(\mathbf{r}-\mathbf{r}', t-t') \\ &\times \cos\left[\frac{pF}{\gamma}(t-t')\right], \end{aligned} \quad (\text{A37c})$$

$$\begin{aligned} \Delta S(\lambda) &= \frac{1}{4} p^5 g^2 \int d\mathbf{r} dt i \tilde{u}^<(\mathbf{r}, t) \{-[\nabla u^<(\mathbf{r}, t)]^2\} \\ &\times \int d\mathbf{r}' dt' (\mathbf{r}-\mathbf{r}')^2 \mathcal{K}(\mathbf{r}-\mathbf{r}', t-t') \\ &\times \sin\left[\frac{pF}{\gamma}(t-t')\right], \end{aligned} \quad (\text{A37d})$$

$$\begin{aligned} \Delta S(F) &= \frac{1}{2} p^3 g^2 \int d\mathbf{r} dt i \tilde{u}^<(\mathbf{r}, t) \int d\mathbf{r}' dt' \mathcal{K}(\mathbf{r}-\mathbf{r}', t-t') \\ &\times \sin\left[\frac{pF}{\gamma}(t-t')\right]. \end{aligned} \quad (\text{A37e})$$

Here we pause a moment to indicate that if we use the complete expression of the kernel $\mathcal{K}(\mathbf{r}, t)$

$$\mathcal{K}(\mathbf{r}, t) = e^{-(1/2)p^2 C_0^>(\mathbf{r}, t)} R_0^>(\mathbf{r}, t) \quad (\text{A38})$$

into Eq. (A37e) and let $b \rightarrow \infty$, then we obtain from Eq. (A37e) above the following expression for the friction force F_{fr} due to the pinning potential to order g^2 :

$$\begin{aligned} F_{fr} &= \frac{1}{2} p^3 g^2 \int d\mathbf{r}' dt' e^{-(1/2)p^2 C_0(\mathbf{r}-\mathbf{r}', t-t')} \\ &\times R_0(\mathbf{r}-\mathbf{r}', t-t') \sin\left[\frac{pF}{\gamma}(t-t')\right], \end{aligned} \quad (\text{A39})$$

which leads directly to the perturbative result (3.5) of the text.

We now go back to our dynamic RG recursion relations (A37a)–(A37e). In the dynamic kernels of Eqs. (A29) and (A30), we expand

$$\tilde{\mathcal{K}}(\mathbf{r}, t) = -p^2 G_0^>(\mathbf{r}, t) - \frac{1}{4} p^4 [G_0^>(\mathbf{r}, t)]^2, \quad (\text{A40a})$$

$$\mathcal{K}(\mathbf{r}, t) = R_0^>(\mathbf{r}, t) - \frac{1}{2} p^2 C_0^>(\mathbf{r}, t) R_0^>(\mathbf{r}, t), \quad (\text{A40b})$$

and keep only the second term⁸² on the rhs of the above equations [the first term gives a vanishing contribution, for reasons which are identical to those explained after Eq. (A16) of Sec. 1]. Now, from Eqs. (A37b)–(A37e), we see that the perturbative corrections to the bare parameters of the theory are given by the flows

$$\left. \frac{d(\gamma T)}{d\ell} \right|_{pert} = \frac{T\lambda^2}{8\pi K^3} + p^2 g^2 \int d\mathbf{r} dt \tilde{\mathcal{K}}(\mathbf{r}, t) \cos\left(\frac{pF}{\gamma} t\right),$$

$$\left. \frac{d\gamma}{d\ell} \right|_{pert} = \frac{1}{2} p^4 g^2 \int d\mathbf{r} dt \mathcal{K}(\mathbf{r}, t) \cos\left(\frac{pF}{\gamma} t\right),$$

$$\left. \frac{dK}{d\ell} \right|_{pert} = \frac{1}{4} p^4 g^2 \int d\mathbf{r} dt r^2 \mathcal{K}(\mathbf{r}, t) \cos\left(\frac{pF}{\gamma} t\right),$$

$$\left. \frac{d\lambda}{d\ell} \right|_{pert} = \frac{1}{4} p^5 g^2 \int d\mathbf{r} dt r^2 \mathcal{K}(\mathbf{r}, t) \sin\left(\frac{pF}{\gamma} t\right),$$

$$\left. \frac{dF}{d\ell} \right|_{pert} = \frac{1}{2} p^3 g^2 \int d\mathbf{r} dt \mathcal{K}(\mathbf{r}, t) \sin\left(\frac{pF}{\gamma} t\right).$$

Using Eqs. (A40a) and (A40b), the above recursion relations become

$$\frac{d}{d\ell}(\gamma T) = \left[\frac{T\lambda^2}{8\pi K^3} + \frac{Tp^6 g^2}{16\pi K^3 \Lambda^4} \frac{1}{1+f^2} \right] (\gamma T), \quad (\text{A41a})$$

$$\frac{d\gamma}{d\ell} = \frac{Tp^6 g^2}{16\pi K^3 \Lambda^4} \frac{1-f^2}{(1+f^2)^2} \gamma, \quad (\text{A41b})$$

$$\frac{dg}{d\ell} = \left(2 - \frac{Tp^2}{4\pi K} \right) g, \quad (\text{A41c})$$

$$\frac{dK}{d\ell} = \frac{Tp^6 g^2}{16\pi K^2 \Lambda^4} \frac{2-3f^2-f^4}{(1+f^2)^3}, \quad (\text{A41d})$$

$$\frac{d\lambda}{d\ell} = \frac{Tp^7 g^2}{16\pi K^2 \Lambda^4} \frac{f(f^2+5)}{(1+f^2)^3}, \quad (\text{A41e})$$

$$\frac{dF}{d\ell} = \frac{\lambda T \Lambda^2}{4\pi K} - \frac{Tp^5 g^2}{8\pi K^2 \Lambda^2} \frac{f}{1+f^2}. \quad (\text{A41f})$$

On the other hand, we know from Eqs. (4.12a)–(4.13) that the rescaling of fields and space and time variables produces the recursion relations

$$\left. \frac{d(\gamma T)}{d\ell} \right|_{resc} = \left. \frac{d\gamma}{d\ell} \right|_{resc} = \left. \frac{dK}{d\ell} \right|_{resc} = \left. \frac{d\lambda}{d\ell} \right|_{resc} = 0,$$

$$\left. \frac{dF}{d\ell} \right|_{resc} = 2F. \quad (\text{A41g})$$

Using the recursion relations above along with the fact that, in a renormalization-group transformation,

$$\frac{d}{d\ell} = \left. \frac{d}{d\ell} \right|_{pert} + \left. \frac{d}{d\ell} \right|_{resc}, \quad (\text{A42})$$

leads directly to Eqs. (4.16b)–(4.16f) of the text.

-
- ¹J. Krim and G. Palasantzas, *Int. J. Mod. Phys. B* **9**, 599 (1995).
²M. Kardar, lectures given at the the Fourth CTP Workshop on Statistical Physics, Seoul National University, Korea; cond-mat/9704172 (unpublished).
³G. Grüner, *Rev. Mod. Phys.* **60**, 1129 (1988).
⁴G. Blatter, M.V. Feigelman, V.B. Geshkenbein, A.I. Larkin, and V.M. Vinokur, *Rev. Mod. Phys.* **66**, 1125 (1994).
⁵T. Giamarchi and P. Le Doussal, *Phys. Rev. Lett.* **76**, 3408 (1996); *Phys. Rev. B* **57**, 11 356 (1998).
⁶L. Balents, M.C. Marchetti, and L. Radzihovsky, *Phys. Rev. Lett.* **78**, 751 (1997); *Phys. Rev. B* **57**, 7705 (1998).
⁷S. Scheidl and V.M. Vinokur, *Phys. Rev. B* **57**, 13 800 (1998).
⁸E.A. Andrei, G. Deville, D.C. Glatli, F.I.B. Williams, E. Paris, and B. Etienne, *Phys. Rev. Lett.* **60**, 2765 (1988).
⁹D.S. Fisher, K. Dahmen, S. Ramanathan, and Y. Ben-Zion, *Phys. Rev. Lett.* **78**, 4885 (1997).
¹⁰M. O. Robbins and M. H. Müser, in *Handbook of Modern Tribology*, edited by Bharat Bhushan (CRC Press, Boca Raton, 2000).
¹¹K. Binder and A.P. Young, *Rev. Mod. Phys.* **58**, 801 (1986).
¹²J.G. Bednorz and K.A. Müller, *Z. Phys.* **64**, 189 (1986).
¹³D.S. Fisher, M.P.A. Fisher, and D.A. Huse, *Phys. Rev. B* **43**, 130 (1991).
¹⁴D.S. Fisher, *Phys. Rev. Lett.* **56**, 1964 (1986).
¹⁵T. Nattermann, *Phys. Rev. Lett.* **64**, 2454 (1990); S.E. Korshunov, *Phys. Rev. B* **48**, 3969 (1993); T. Giamarchi and P. Le Doussal, *Phys. Rev. Lett.* **72**, 1530 (1994); *Phys. Rev. B* **52**, 1242 (1995); T. Emig, S. Bogner, and T. Nattermann, *Phys. Rev. Lett.* **83**, 400 (1999).
¹⁶T. Nattermann and S. Scheidl, *Adv. Phys.* **49**, 607 (2000).
¹⁷L. Balents and D.S. Fisher, *Phys. Rev. B* **48**, 5949 (1993).
¹⁸L. Radzihovsky and J. Toner, *Phys. Rev. Lett.* **81**, 3711 (1998).
¹⁹S. Bhattacharya and M.J. Higgins, *Phys. Rev. Lett.* **70**, 2617 (1993); *Phys. Rev. B* **52**, 64 (1995); M.J. Higgins and S. Bhattacharya, *Physica C* **257**, 232 (1996).
²⁰L.W. Chen, L. Balents, M.P.A. Fisher, and M.C. Marchetti, *Phys. Rev. B* **54**, 12 798 (1996).
²¹A. Schmid and W. Hauger, *J. Low Temp. Phys.* **11**, 667 (1973).
²²A.A. Middleton, *Phys. Rev. Lett.* **68**, 670 (1992).
²³O. Narayan and D.S. Fisher, *Phys. Rev. B* **46**, 11 520 (1992).
²⁴A.A. Middleton, *Phys. Rev. B* **45**, 9465 (1992).
²⁵D.S. Fisher and D. Huse, *Phys. Rev. B* **38**, 373 (1988); **38**, 386 (1988).
²⁶L.B. Ioffe and V.M. Vinokur, *J. Phys. C* **20**, 6149 (1987).
²⁷M.V. Feigel'man, V.B. Geshkenbein, A.I. Larkin, and V.M. Vinokur, *Phys. Rev. Lett.* **63**, 2303 (1989).
²⁸T. Nattermann, *Phys. Rev. Lett.* **64**, 2454 (1990).
²⁹Y.C. Tsai and Y. Shapir, *Phys. Rev. E* **50**, 4445 (1994).
³⁰L. Radzihovsky, *Proceedings of the American Physical Society* (talk E37 8), 1998 (unpublished); L. Balents, D. S. Fisher, and L. Radzihovsky (unpublished).
³¹P. Chauve, T. Giamarchi, and P. Le Doussal, *Europhys. Lett.* **44**, 110 (1998).

- ³²L. Balents, D. S. Fisher, and L. Radzihovsky (unpublished).
- ³³L. Balents and P. Le Doussal, cond-mat/0205358.
- ³⁴P.E. Wolf, F. Gallet, S. Balibar, E. Rollet, and Ph. Nozières, *J. Phys. (France)* **46**, 1987 (1985).
- ³⁵A. Chowdhury, B.J. Ackerson, and N.A. Clark, *Phys. Rev. Lett.* **55**, 833 (1985), and references therein.
- ³⁶Q.-H. Wei, C. Bechinger, D. Rudhardt, and P. Leiderer, *Phys. Rev. Lett.* **81**, 2606 (1998).
- ³⁷E. Frey, D.R. Nelson, and L. Radzihovsky, *Phys. Rev. Lett.* **83**, 2977 (1999).
- ³⁸L. Radzihovsky, E. Frey, and D.R. Nelson, *Phys. Rev. E* **63**, 031503 (2001).
- ³⁹See, for example, C. Reichhardt, and C.J. Olson, cond-mat/0201258 (unpublished); cond-mat/0201021 (unpublished).
- ⁴⁰M.C. Marchetti, A.A. Middleton, and T. Prellberg, *Phys. Rev. Lett.* **85**, 1104 (2000).
- ⁴¹J.V. José, L.P. Kadanoff, S. Kirkpatrick, and D.R. Nelson, *Phys. Rev. B* **16**, 1217 (1977); **17**, 1477(E) (1978).
- ⁴²S.T. Chui and J.D. Weeks, *Phys. Rev. B* **14**, 4978 (1976); *Phys. Rev. Lett.* **40**, 733 (1978).
- ⁴³P.B. Wiegmann, *J. Phys. C* **11**, 1583 (1978).
- ⁴⁴T. Ohta and D. Jasnow, *Phys. Rev. B* **20**, 139 (1979).
- ⁴⁵D.J. Amit, Y.Y. Goldshmidt, and G. Grinstein, *J. Phys. A* **13**, 585 (1980).
- ⁴⁶H.J.F. Knops and L.W.J. den Ouden, *Physica A* **103**, 597 (1980).
- ⁴⁷B. Neudecker, *Z. Phys. B: Condens. Matter* **49**, 57 (1982).
- ⁴⁸P. Nozières and F. Gallet, *J. Phys.* **48**, 353 (1987).
- ⁴⁹M. Rost and H. Spohn, *Phys. Rev. E* **49**, 3709 (1994).
- ⁵⁰H. von Beijeren, *Phys. Rev. Lett.* **38**, 993 (1977).
- ⁵¹T. Hwa, M. Kardar, and M. Paczuski, *Phys. Rev. Lett.* **66**, 441 (1991).
- ⁵²M. Kardar, G. Parisi, and Y. C Zhang, *Phys. Rev. Lett.* **56**, 889 (1986).
- ⁵³The situation here is quite analogous to the lack of qualitative distinction and therefore to the rounding of the phase transition between a paramagnetic and ferromagnetic phases in the presence of a finite external magnetic field H , with magnetization $M(H)$ finite in both phases. Nevertheless, in the limit of a vanishing field, the equation of state $M(H, T)$ displays a qualitatively distinct behavior as a function of H , exhibiting a diverging differential susceptibility for $T < T_c$ and a finite one for $T > T_c$.
- ⁵⁴R. Seshadri and R.M. Westervelt, *Phys. Rev. B* **46**, 5142 (1992); **46**, 5150 (1992).
- ⁵⁵M.P.A. Fisher, *Phys. Rev. Lett.* **62**, 1415 (1989).
- ⁵⁶Saito, *Z. Phys. B* **32**, 75 (1978).
- ⁵⁷L. Landau and E. Lifshitz, *Statistical Physics* (Clarendon Press, Oxford, 1938).
- ⁵⁸W.K. Burton, N. Cabrera, and F.C. Frank, *Philos. Trans. R. Soc. London, Ser. A* **243**, 299 (1951).
- ⁵⁹L. Sneddon, M.C. Cross, and D.S. Fisher, *Phys. Rev. Lett.* **49**, 292 (1982).
- ⁶⁰H. Risken, *The Fokker-Planck Equation* (Springer, Berlin, 1984).
- ⁶¹S. Scheidl, *Z. Phys. B: Condens. Matter* **97**, 345 (1995).
- ⁶²A. P. Prudnikov, Yu. A. Brychkov, and O. I. Marychev, *Integrals and Series* (Gordon and Breach, New York, 1986).
- ⁶³Strictly speaking, these changes all take place even at short scales even before a continuum limit is reached. Consequently, at continuum level they are already present, and a careful coarse-graining procedure on the *discrete* lattice model must be done to derive the continuum nonequilibrium model as was done in Ref. 6.
- ⁶⁴B.I. Halperin, P.C. Hohenberg, and S.K. Ma, *Phys. Rev. Lett.* **29**, 1548 (1972).
- ⁶⁵P.C. Hohenberg and B.I. Halperin, *Rev. Mod. Phys.* **49**, 435 (1977).
- ⁶⁶S. Ma, *Modern Theory of Critical Phenomena* (Benjamin, New York, 1976).
- ⁶⁷P.C. Martin, E.D. Siggia, and H.A. Rose, *Phys. Rev. A* **8**, 423 (1973); H.K. Janssen, *Z. Phys. B* **23**, 377 (1976); C. De Dominicis and L. Peliti, *Phys. Rev. B* **18**, 353 (1978); R.V. Jensen, *J. Stat. Phys.* **25**, 183 (1981).
- ⁶⁸The choice of the rescaling exponents z , $\hat{\chi}$ and the phonon field-rescaling exponent ϕ is of course completely arbitrary. If instead of the convenient $z=2$, $\hat{\chi}=-2$, and $\phi=0$ choice, we left them arbitrary, then to return the Hamiltonian into the form it had before the RG transformation, we would instead find that $K(b)$, $\gamma(b)$, and the wave vector $p(b)=pb^\phi$ flow even at the lowest order. It is easy to check that the flow equations for the *dimensionless* couplings involve $K(b)$, $\gamma(b)$, and $p(b)$ and are independent of the arbitrary choice of z , $\hat{\chi}$, and ϕ .
- ⁶⁹Y. Saito, *Statistical Physics of Crystal Growth* (World Scientific, Singapore, 1996).
- ⁷⁰J.M. Kosterlitz and J.M. Thouless, *J. Phys. C* **6**, 1181 (1973).
- ⁷¹D.R. Nelson and J.M. Kosterlitz, *Phys. Rev. Lett.* **39**, 1201 (1977).
- ⁷²J. Villain, *J. Phys. (Paris)* **36**, 581 (1975).
- ⁷³E. Frey, D.R. Nelson, and L. Radzihovsky, *Phys. Rev. Lett.* **83**, 2977 (1999); L. Radzihovsky, E. Frey, and D.R. Nelson, *Phys. Rev. E* **63**, 031503 (2001).
- ⁷⁴R.G. Petschek and A. Zippelius, *Phys. Rev. B* **23**, 3483 (1981).
- ⁷⁵A.E. Koshelev and V.M. Vinokur, *Phys. Rev. Lett.* **73**, 3580 (1994).
- ⁷⁶*Handbook of Mathematical Functions*, edited by M. Abramowitz and I. A. Stegun, (Dover, New York, 1972).
- ⁷⁷M.-C. Cha and H.A. Fertig, *Phys. Rev. Lett.* **80**, 3851 (1998).
- ⁷⁸C. Reichhardt, C.J. Olson, and F. Nori, *Phys. Rev. Lett.* **78**, 2648 (1997); *Phys. Rev. B* **57**, 7937 (1998); C. Reichhardt and F. Nori, *Phys. Rev. Lett.* **82**, 414 (1999); V. Gotcheva and S. Teitel, *ibid.* **86**, 2126 (2126).
- ⁷⁹K.G. Wilson and J. Kogut, *Phys. Rep.* **12**, 75 (1974).
- ⁸⁰F.J. Wegner and A. Houghton, *Phys. Rev. A* **8**, 401 (1973).
- ⁸¹J.B. Kogut, *Rev. Mod. Phys.* **51**, 659 (1979).
- ⁸²There has been considerable confusion in the literature (Ref. 48) over the graphical correction to the elastic stiffness K . The most common source of the confusion is the use of a soft cutoff scheme in which there is an apparent correction to K coming from an expansion of the exponential in Eq. (A15) to first order in $G_{>}(\mathbf{r})$. Such correction clearly vanishes in the sharp cutoff momentum-shell scheme that we employ here because it is proportional to $\nabla_{\mathbf{q}}^2 G_{>}(\mathbf{q})|_{\mathbf{q}=0}$ which is identically zero in this scheme. Such linear in $G_{>}$ non-1PI correction also reassuringly vanishes in field-theoretic approaches in which only 1PI graphs must be kept. The most compelling argument against using any scheme that gives a linear in $G_{>}$ correction is that such terms lead to corrections to coupling constants that are independent of temperature and therefore survive in the $T \rightarrow 0$ limit. Clearly,

such terms cannot contribute to fluctuation-driven renormalization of model parameters. However, near T_c the only universal part of the correction to K is its quadratic dependence on g , with the coefficient of g^2 only affecting the nonuniversal quantities such as α in Eq. (4.35b), but leaving universal details, like the

exponent $1/2$ of ξ and the universal jump at T_c of the ratio K/T unchanged. It is for this reason that conceptually erroneous calculations can and have gotten away with reproducing the usual sine-Gordon (KT) phenomenology.

⁸³T. Nattermann and L.-H. Tang, Phys. Rev. A **45**, 7156 (1992).